Title: Optimisation can provide the fundamental link between leaf photosynthesis, gas exchange and water relations.

Authors: Ross M. Deans[1], Timothy J. Brodribb[2], Florian A. Busch[1,3] and Graham D. Farquhar[1].

[1]ARC Centre of Excellence in Translational Photosynthesis, Division of Plant Science, Research School of Biology, The Australian National University, Canberra, ACT 2601, Australia; [2]School of Biological Sciences, University of Tasmania, Hobart, TAS 7001, Australia; [3]School of Biosciences, University of Birmingham, Birmingham, UK.

Author ORCID iD: Ross M. Deans: 0000-0003-3831-2520; Timothy J. Brodribb: 0000-0002-4964-6107; Florian A. Busch: 0000-0001-6912-0156; Graham D. Farquhar: 0000-0002-7065-1971

Author for correspondence:
Graham D. Farquhar
Tel: +61 2 6125 3743
Email: Graham.Farquhar@anu.edu.au

Abstract

Tight coordination in the photosynthetic, gas exchange and water supply capacities of leaves is a globally conserved trend across land plants. Strong selective constraints on leaf carbon gain create the opportunity to use quantitative optimisation theory to understand the connected evolution of leaf photosynthesis and water relations. We developed an analytical optimisation model that maximises the long-term rate of leaf carbon gain, given carbon costs in building and maintaining stomata, leaf hydraulics and osmotic pressure. Our model demonstrates that selection for optimal gain should drive coordination between key photosynthetic, gas exchange and water relations traits. It also provides predictions of adaptation to drought and the relative costs of key leaf functional traits. Our results show that optimisation in terms of carbon gain given carbon costs of physiological traits successfully unites leaf photosynthesis and water relations and provides a quantitative framework to consider leaf functional evolution and adaptation.

Introduction

Maintaining net positive carbon gain at the leaf level represents a finely balanced economic challenge to the plant: the beneficial uptake of CO_2 through stomata for photosynthesis is coupled to a large cost in terms of the unavoidable loss of typically 100-fold more water to the atmosphere. To maximise reproductive gain and avoid death through desiccation, plants must adopt the best strategy, both in short-term

47 behaviour and long-term investment in physiological traits, to succeed in a
48 challenging and competitive environment.
49 Optimisation provides an intuitive, theoretical basis to uncover what the best strategy
50 may be. It posits that in a population of individuals, those that exhibit optimal
51 behaviour will have a relatively greater carbon gain over their life than those that are
52 not optimal. Thus natural selection should act to shift a population towards greater
53 carbon gain, insofar as greater carbon gain is associated with increased fitness [1-3].
54 Provided plants are behaving optimally, predictions from optimisation theory can
55 provide insights into what processes are of fundamental importance to plants, as well
56 as the costs of these functionally important components.
57 The leaf is the main plant organ responsible for photosynthetic carbon gain and as
58 such the long-term adaptive coordination of leaf physiological traits across species is
59 globally significant [4]. It has also made leaves an integral component in understanding
60 whole-plant fitness in terms of maximising carbon gain. For example, the
61 coordination between light-saturated photosynthesis (measured as light-saturated CO_2
62 assimilation rate, A_{sat}) and the light-saturated leaf surface porosity to gas exchange
63 through stomata (measured as light-saturated stomatal conductance, g_{sat}) represents a
64 conservative global feature of plant behaviour [5,6]. Remarkably, optimisation theory
65 pre-empted the discovery of the coordination of CO_2 assimilation rate and leaf surface
66 porosity [2,7,8] by considering the economic gains of CO_2 assimilation for the loss of
67 transpiration by two different approaches, later shown to be equivalent [3]. Farquhar [7]
68 and Givnish and Vermeij [9] considered that there was an inherent metabolic cost of
69 transpiration, and that plants would possess a leaf surface porosity that would
70 maximise the difference between CO_2 assimilation and the transpiration cost. Cowan
71 and Farquhar [2] instead suggested plants would possess a leaf surface porosity that

would minimise the transpiration lost for a given amount of photosynthesis gained. However, it is not intuitive how the metabolic cost of transpiration [9] and the marginal cost of water [2] directly relate to physical plant traits.

New insights into the limitations on plant gas exchange have come from considering the "supply" end of the transpiration pathway. The inevitable loss of transpiration associated with carbon assimilation must ultimately be balanced by the supply of liquid water to the leaves [10]. The size of this flux at the leaf level is determined by two factors: the ease of movement of liquid water through the leaf (measured as leaf hydraulic conductance, K_{leaf}), and the difference in water potential ($\Delta\Psi$) between the stem and the leaf [10]. Leaves are major resistors to water flow in the whole plant [11], exerting a disproportionate influence over maximum water supply. Thus altering K_{leaf} or $\Delta\Psi$ represent two divergent strategies that plants could adopt to supply the increased transpiration optimally demanded for an increase in A_{sat}.

Vascular plants show tight coordination between K_{leaf}, g_{sat} and A_{sat} across species [12-14], resulting in a diversity of species occupying a surprisingly conserved range of leaf water potentials under well-watered conditions [15]. Coordination between K_{leaf} and g_{sat} could represent a balanced allocation of resources [10] and/or constrain variation in $\Delta\Psi$ under varying environmental conditions, reducing the risk of damage to the water transport system by excessive hydraulic tension [16]. However, given the diversity across vascular plants in the capacity of the water transport tissue (xylem) to cope with large variations in $\Delta\Psi$ [17], it is perhaps surprising that selection would favour adapting water supply by changing K_{leaf} rather than adapting $\Delta\Psi$.

Optimisation may provide the fundamental rationale for the coordination of K_{leaf}, g_{sat} and A_{sat}. There has been a wealth of studies that successfully extend optimisation ideas to directly or indirectly include liquid phase transport, predominantly at the

97 whole-plant level. These can be broadly split into formulations that model stomatal
98 responses to environmental stimuli [1,18-23], and those that model the coordination of
99 traits at a tissue[24], organ [25] or whole-plant level [26-29]. Many formulations either: (1)
100 require predominantly numerical solutions, which limit an intuitive understanding of
101 the underlying causes and effects; (2) optimise by considering variations in leaf
102 surface porosity only, which limits the utility of optimisation for the estimation of
103 relative costs of physiological traits; or (3) consider the optimisation of few
104 physiological traits, rarely including liquid-phase conductance as a predicted
105 outcome.
106 Here we evaluate whether observations of coordination between photosynthetic, gas
107 exchange and hydraulic systems in leaves conforms to an optimal model of resource
108 acquisition. We do so by developing an analytic optimisation model that integrates
109 photosynthetic physiology with diffusive and liquid flow properties of the whole leaf
110 and simultaneously optimises for a number of leaf traits. The optimisation model
111 maximises overall carbon gain by allocating investments in functional traits required
112 to support gas exchange for photosynthesis. These investments entail carbon costs for
113 both the construction and maintenance of traits. The key leaf costs considered are of
114 stomata, hydraulics and osmotic pressure, with the relation between these investments
115 and plant carbon-water balance linked by physiology (Fig. 1). The optimisation is
116 considered to occur over a sufficiently long timescale to encompass a number of
117 cycles of leaf replacement. As such, it does not explicitly consider short-term dynamic
118 plant responses, but rather it considers average investments and returns of carbon
119 under average growth conditions. Variation between species is prescribed by a
120 linearised biochemical photosynthetic capacity (k; see Methods) but is more naturally
121 expressed through A_{sat}, the capacity of photosynthetic carbon income for the leaf

under light-saturated conditions. Expressing trait variation in terms of photosynthetic carbon income is common in both experimental [5,6,13] and modelling studies [30-32]. We show that this analytical, optimisation model simultaneously predicts a number of fundamental relationships between photosynthesis, gas exchange and plant water relations, and how physiological traits vary in the long-term under different environmental conditions. Moreover, fitting of the model to observed species data provides estimates of the relative costs of physiological traits required to support photosynthesis without the need for detailed, mechanistic accounting of the energetic or structural costs of traits, provided plants are optimally configured.

Results

The analytical optimisation model provided five key predictions (see Methods). The first four assume that cost parameters for stomata, hydraulics and osmotic pressure are relatively conserved across species. The predictions are:

(1) leaf osmotic pressure at turgor loss point (π_{tlp}) is independent of photosynthesis and is set only by the conditions of leaf water availability and evaporative demand to which plants are adapted (equation 26);

(2) leaf liquid-phase conductance and photosynthesis are coordinated (equation 28);

(3) leaf gas-phase conductance and photosynthesis are coordinated (equation 29);

(4) stem to leaf water potential difference is independent of photosynthesis (equation 30);

(5) relative costs of stomata, hydraulics and osmotic pressure can be estimated from data (equations 31-33).

147

148 The optimisation model predicted that both stomatal conductance and leaf hydraulic
149 conductance should be linearly proportional to assimilation rate under constant
150 environmental conditions. Predicting linear coordination between g_{sat} and A_{sat} was
151 identical to predicting a conserved leaf internal CO_2 concentration (C_i) across species
152 (see equations 7 and 29). The model was effective at explaining the observed
153 coordination between measured g_{sat} and A_{sat} across species (fitting set $R^2 = 0.66$, full
154 set $R^2 = 0.61$; Fig. 2a), particularly over the linear region encompassing low to
155 moderate A_{sat}. It could not explain why measured g_{sat} tended to increase more rapidly
156 than linearly at higher A_{sat}. Importantly however, the optimisation model captured the
157 strong linear correlation between K_{leaf} and A_{sat} observed across species (Fig. 2b; fitting
158 set $R^2 = 0.83$, full set $R^2 = 0.89$).
159 There was no relationship between $\Delta\Psi$ and A_{sat}, and $\Delta\Psi$ was not significantly
160 different in the sample species from that calculated from the optimisation model
161 (predicted $\Delta\Psi = 0.29$ MPa, one-sample t-test $P = 0.27$; Fig. 2c).
162 The optimisation model predicted that, across species, leaf osmotic pressure should be
163 independent of assimilation rate and constant under identical environmental
164 conditions. However, data from 16 species ranging from lycophytes to angiosperms
165 showed a weak, significant relation between osmotic pressure and A_{sat}, despite
166 apparent conservatism in π_{tlp} at lower photosynthetic rates (Fig. 2d; $R^2 = 0.28$, $P =$
167 0.021).
168 Optimal A_{sat}, g_{sat}, K_{leaf}, π_{tlp} and $\Delta\Psi$ were modelled for a range of leaf to air water mole
169 fraction difference (Δw) and leaf source water potential (Ψ_s) to simulate adaptation to
170 mean atmospheric dryness and leaf petiole water potential, respectively (Fig. 3). The
171 latter combined the effects of both soil dryness and other plant resistances to water

172 flow on leaf water potential. The simulations used the mean across species of the cost
173 parameter for each trait and assumed a given biochemical photosynthetic capacity (k,
174 a linearised form of the maximum carboxylation rate of Rubisco; see Methods).
175 Predicted A_{sat} and g_{sat} were relatively conserved across a range of Δw and Ψ_s (Fig. 3a-
176 d), but the reason for this differed depending on whether Δw or Ψ_s provided the
177 environmental variation. Both adaptive K_{leaf} and $\Delta\Psi$ were predicted to increase under
178 drier atmospheric conditions to supply greater transpiration, while there was little
179 predicted shift in π_{tlp} (Fig. 3e, 3g and 3i). In contrast, adaptive π_{tlp} was predicted to
180 increase under drier source water conditions, while predicted K_{leaf} and $\Delta\Psi$ were
181 relatively conserved (Fig. 3f, 3h and 3j). Optimal adaptive A_{sat} and g_{sat} both showed
182 much weaker sensitivities over a range of Δw than that predicted from the Cowan-
183 Farquhar stomatal optimisation model (Fig. 3a and 3c).
184 Our optimisation model provided a means to estimate the costs of hydraulics, stomata
185 and osmotic pressure for a leaf, relative to the combined cost of the three traits. Leaf
186 hydraulics were estimated to contribute 10.0 ± 1.1% of the combined cost of the three
187 traits, while stomata were estimated to contribute 43.3 ± 1.2% and osmotic pressure
188 46.7 ± 0.2% (Fig. 4; hydraulics-stomata: $P = 4.5 \times 10^{-4}$, hydraulics-osmotic pressure:
189 $P = 1.1 \times 10^{-8}$, stomata-osmotic pressure: n.s.).
190
191
192 Discussion
193
194 The coordination between leaf gas exchange and hydraulic capacities across species
195 represents a fundamental crossover between plant productivity and leaf water
196 relations [10]. Here we have shown that optimisation to maximise carbon gain at the leaf

197 level provides a strong theoretical rationale that can explain key adaptive trends
198 observed in stomatal, hydraulic and leaf osmotic traits across species. This is
199 significant as it provides a quantitative explanation for the coordination between
200 photosynthesis, gas exchange and leaf water relations, in terms of maximising carbon
201 gain.
202 Predicting the coordination between photosynthesis and leaf hydraulic conductance
203 represents a major success of our optimisation model. Coordination between
204 photosynthetic rate and stomatal conductance has previously been shown to be
205 optimal in terms of the water-carbon economy of the plant [2,30,32]. However, further
206 coordination of liquid and vapour water conductances has only been informally
207 discussed as a balanced allocation of resources [10], or as a means of constraining $\Delta\Psi$ to
208 avoid xylem cavitation [16]. Our optimisation model quantitatively supports the
209 coordination of photosynthesis and hydraulics as representing the most efficient use
210 of resources.
211 It is of interest that no direct specification of xylem vulnerability to cavitation was
212 required to produce observed trends. There is debate about whether the liquid-phase
213 conductance to water in aerial plant tissues decreases appreciably with decreases in
214 tissue water potential over the range where stomata are open [33-35], or whether
215 hydraulic conductance predominantly decreases at water potentials drier than the
216 point of stomatal closure [36-39]. We took the simpler assumption of hydraulic
217 conductance remaining largely constant over the range of water potentials where
218 stomata are open. This is a potential limitation of our model; however, that our model
219 can explain observed trends in the leaf traits here supports our choice of assumptions.
220 A second remarkable outcome of the model is the inclusion of osmotic pressure at
221 turgor loss point, a fundamental trait in the understanding of leaf water relations, as an

emergent trait from maximising carbon gain. The role of osmotic pressure at turgor loss point in maintaining leaf turgor and stomatal opening for active photosynthesis has been qualitatively described numerous times, particularly its importance under drier conditions [40-42]. Our optimisation model provides support for this important mechanism, quantitatively linking leaf osmotic pressure at turgor loss point with gas exchange and the leaf carbon economy.

Tight coordination of leaf liquid and vapour conductances theoretically leads to constant stem to leaf water potential differences across species under constant environmental conditions [10]. Both our optimisation model and the species data support the conservation of stem to leaf water potential differences across different photosynthetic capacities under well-watered, saturating light conditions, when plants have been adapted to similar environmental conditions. This contrasts with other studies that have shown either greater [14] or decreased [43] gradients in stem to leaf water potential with increasing photosynthetic capacity. However, as the measured species are representative of a broad range of environments and measurement conditions, while the model fitting assumed identical environmental conditions across species, some deviation between the model and observations is expected.

Measured g_{sat} increased more rapidly than linearly for high A_{sat} across species, such that species became less water-use efficient at higher gas exchange rates [14,44]. This could come about if the carbon cost of stomata becomes marginally cheaper the denser they are packed on the leaf surface. Optimal allocation of the leaf surface area to stomata requires that higher g_{sat} be achieved with smaller, more-densely distributed stomata [45,46]. If smaller stomata are individually less costly than larger stomata [47] then this could lead to the overall cost of stomata becoming marginally cheaper the denser they are on the leaf surface. Our model effectively assumes all stomata to be of equal

size and cost and so will not capture this sort of behaviour. A similar effect in K_{leaf} might also be expected based on the vein cost of K_{leaf} becoming marginally cheaper at higher vein densities in leaves with reticulate venation [48], but was only weakly observed in this dataset, and suggests anatomical determinants of K_{leaf} other than vein density, such as leaf depth or mesophyll properties, may be playing a modifying role [13,48-50]. If the marginal costs of small, dense stomata decrease more rapidly than those for denser venation networks, then stomatal conductance could increase relatively more than leaf hydraulic conductance for an increase in photosynthetic capacity. In this situation increases in hydrodynamic pressure gradients with increased photosynthetic capacity would be expected [14]. This could also explain the weak but significant trend of increasing π_{tlp} with increasing photosynthetic capacity observed in the dataset presented here.

Our model employs a linearised approximation for photosynthetic biochemistry; however, it is unlikely that using the full nonlinear representation of photosynthesis of Farquhar, et al. [51] would provide a better prediction for the A_{sat} and g_{sat} relation when photosynthetic capacity is the only source of variation. For example, Arneth, et al. [52] derived equations for the Cowan and Farquhar [2] optimisation but included the nonlinear photosynthesis equation, again predicting a linear relation between A_{sat} and g_{sat} when photosynthetic capacity is the source of variation. This is because CO_2 assimilation rate behaves linearly when both photosynthetic capacity and stomatal conductance change proportionally and boundary layer conductance is ignored [53,54]. It may be that better predictions of the coordination between assimilation and leaf gas exchange conductance could be achieved if the more physically relevant total conductance to CO_2 were used. However, an optimisation model including boundary layer conductance would require inclusion of the feedback of transpiration on leaf

272 temperature [8] and the impact of leaf size on boundary layer [9], both reducing the
273 analytic tractability of the model.
274 The optimisation model predicts different adaptive strategies under water-stressed
275 conditions, depending on whether water stress occurs via high evaporative demand
276 (Δw) or because of drier petiole water potential (Ψ_s). Our model suggests that
277 adaptive shifts to accommodate drier environments are a combination of greater
278 investments in veins under drier atmospheres [55] and greater leaf osmotic pressures in
279 drier soils [56,57], inasmuch as drier soils would manifest themselves as drier petiole
280 water potentials. It should be noted that natural water stresses from evaporative
281 demand and petiole water potential are dynamic, not static as assumed in our model,
282 and are likely to co-occur. Dynamic water stress may also modify the effective
283 fraction of time that plants are active and provide additional selective pressures for
284 plant survival, while biochemical photosynthetic capacity is also likely to be
285 environment-dependent. We then caution that the illustrated trends in response to
286 water stress should be viewed as being indicative only. However, because these
287 predictions are obtained for a given photosynthetic income, this means that the leaf
288 carbon balance is predicted to be more marginal under drier environments. This
289 would compound the reduced opportunity for photosynthesis caused by soil water
290 deficit driving stomatal closure, contributing to the rapid changes in plant
291 communities that occur across precipitation gradients.
292 Our model does not directly deal with hydraulic vulnerability, but it could still
293 provide some insight into why observed trade-offs between hydraulic efficiency and
294 safety in leaves [58] and stems [59] are weak, and in particular why there is a
295 predominance of species with water supply systems of both low efficiency and low
296 safety [59]. Our results suggest that at the leaf level, photosynthetic capacity sets

297 optimal hydraulic efficiency (the magnitude of K_{leaf}), while π_{tlp} optimally increases
298 under increased source water stress, which has been shown to correlate with the
299 ability of xylem to function under drier water potentials [15,58,60]. Furthermore, scaling
300 of hydraulic flow capacity across the plant vascular system [61,62] and coordination in
301 leaf and stem hydraulic vulnerabilities [63-65] suggests then that leaf and stem hydraulic
302 properties should be coordinated. Thus efficiency and safety of plant hydraulic
303 systems could represent two relatively independent axes of adaptation, the former set
304 by photosynthetic capacity and the latter set by soil dryness. Plants of low efficiency
305 and safety could then reflect those of low photosynthetic capacity adapted to mesic
306 environments [59].
307 Our trait-driven optimisation model also predicts that long-term adaptive A_{sat} and g_{sat}
308 would be relatively conserved for a given biochemical photosynthetic capacity (k)
309 across a large range of average evaporative demand. This is in contrast to both current
310 optimisation [30,32] and hydraulic [31,66,67] models that predict more drastic stomatal
311 closure and loss of photosynthesis in the short-term under the conditions of large
312 evaporative demand. However, a recent study showing maximum stomatal
313 conductance is relatively conserved across biomes [68] may support our model
314 predictions. Conservation of A_{sat} and g_{sat} across evaporative demands could suggest
315 that selection favours different responses for short-term environmental stimuli
316 compared with long-term adaptation to average conditions. Although our model does
317 not include competition for resources, maintaining operational A_{sat} and g_{sat} for a given
318 photosynthetic capacity is more consistent with a competitively favourable strategy,
319 where less-conservative water-use is favoured for greater carbon gain compared with
320 the case without competition [69].The inclusion of competition for resources in

optimisation models is likely to provide a more complex, but complete, picture of plant adaptation under natural conditions [70,71].

A number of simplifying assumptions underpin the model, of which the effect and validity of each are variously known. One key step in the derivation of the model is the condensation of time-averaged photosynthesis in relation to A_{sat} (represented by the effective fraction of time the plant is operating at A_{sat}, f), leaf longevity (τ), and building and maintenance costs for each trait into one overall cost for each trait (equation 4). This step is mathematically robust because neither f nor τ are being optimised. However, we take the further step and assume that there is effectively a common leaf construction motif across plant species. This common construction motif reveals itself in the assumption of constant cost parameters, and so is apparent in underlying assumptions of similar stomatal size, similar xylem hydraulic characteristics and the mesophyll being made of cells of constant photosynthetic nitrogen concentration (see Methods).

The *a priori* assumption of a common leaf construction motif across species seems unlikely to be true in the strict sense. However, the agreement of model predictions with experimental observations suggests that the assumption may provide some useful insights. For example, conservation in cost parameters across species entails higher trait construction costs per leaf area for leaves with greater longevity (equation 4). It would also suggest that the fundamental metabolic costs of building and maintaining physiological traits are approximately conserved across vascular plant lineages, with more minor cost savings appearing from anatomical innovations. Finally, constant cost coefficients across species could suggest that the effective fraction of time that a leaf was photosynthesising at A_{sat} is, on average, approximately constant across species. This is difficult to test, especially when these results reflect long-term

346 evolutionary adaptive traits and not necessarily plastic responses to different light
347 environments. However, it may be consistent with changes of photosynthetic capacity
348 that occur with changes in average irradiance, where decreases in photosynthetic
349 capacity under lower irradiances would act in the direction of conserving *f*.
350 The assumption of a common leaf construction motif implies that the mesophyll is
351 made of cells of constant photosynthetic nitrogen concentration, so that leaf
352 photosynthetic capacity increases with mesophyll depth and that the cost of osmotic
353 pressure is approximately proportional to photosynthetic capacity. The aim of this
354 assumption was to capture how the cost of osmotic pressure could scale with
355 photosynthetic leaf depth, without specifying directly a depth for each species. The
356 assumption is well justified for plastic changes in photosynthetic capacity in response
357 to changes in irradiance but is less well justified for evolutionary differences across
358 species. In the latter case, higher photosynthetic capacities are typically associated
359 with thinner leaves if lower leaf mass per unit area (*LMA*) is a proxy for leaf
360 thickness. However, a distinction should be made between structural aspects of *LMA*
361 that contribute through investments in cell walls, for example, and photosynthetic
362 aspects of *LMA*, as set out in Osnas, et al. [72]. Relating the cost of osmotic pressure to
363 the photosynthetic aspect of *LMA* better captures the dependence of the cost on cell
364 contents, rather than scaling the cost with total leaf depth, which would erroneously
365 include cell wall components. A direct consequence of the cost of osmotic pressure
366 being proportional to photosynthetic capacity is the prediction in the model of π_{tlp}
367 being independent of A_{sat}. It is possible that this assumption is not true in the strict
368 sense and that deviations from it could explain the weak but significant positive
369 relation between π_{tlp} and A_{sat} (Fig. 2d) and the nonlinear dependence of g_{sat} on A_{sat}
370 (Fig. 2a) observed across species. However, the large degree of species variation

observed that the model can capture suggests the assumptions may hold approximately and may provide useful insights into plant functioning.

A major advantage of expressing optimisation in terms of carbon costs of water-relations traits required for photosynthesis is that it provides directly an estimate of the relative costs of the traits, provided plants are behaving optimally. Our model predicts that the costs of both stomata and leaf osmotic pressure are relatively high, while the cost of hydraulics is approximately one quarter of the others (Fig. 4). We interpret the higher costs of stomata and osmotic pressure over hydraulics as representing a division between primarily active maintenance costs for stomata and osmotic pressure, and initial building costs with little associated maintenance for hydraulics. Building the leaf venation system constitutes a major initial carbon cost, but requires relatively little in terms of maintenance costs because the majority of leaf xylem tissue is made up of conduits that are no longer living in mature tissue. In contrast, the continuous maintenance of osmotic gradients between mesophyll cells and the leaf apoplast requires a metabolic cost that could become significant over the lifetime of a leaf [73]. Maintenance of guard cell turgor for gas exchange also entails an active energetic cost [74]. The relatively high metabolic cost of maintaining osmotic pressure is consistent with previous estimates that the maintenance of osmotic gradients could account for 20% of the total maintenance cost in plant tissues [73].

Estimates for the construction costs for leaf hydraulics are more elusive. However, the relative building cost of leaf vasculature spread over the lifespan of the leaf can be crudely estimated from the proportional contribution of leaf mass that is veins [75], mean mass-based construction cost and mean leaf lifespan [76]. The building cost of leaf vasculature per leaf lifespan estimated in this way is approximately 22% of the maintenance cost of osmotic pressure (see Supplementary Methods), surprisingly

close to our optimisation result of 21% of the cost of osmotic pressure. Energetic costs of opening stomata have been estimated based on ionic requirements of guard cell turgor pressure [77,78], but did not consider the energetic requirements of maintaining turgor, while dynamic light environments make mean energetic costs difficult to estimate. We suggest that optimisation could provide estimates of the relative costs of leaf traits, highlighting the hidden costs of leaf maintenance and in particular how potentially costly is the maintenance of stomata and osmotic pressure. Our model has advantages over models that perform optimisation in terms of stomatal conductance (g_s) and not the component traits that make up g_{sat}. For example, Dewar, et al. [18] correctly predicted that optimal g_s should be proportional to $(K_{leaf}A)^{1/2}$ but concluded that g_s would independently co-vary with $K_{leaf}^{1/2}$ and $A^{1/2}$ (where A is the CO_2 assimilation rate). Our trait-based approach provided extra information and showed K_{leaf} itself to be optimally coordinated with A_{sat}, so that the classic optimisation result of g_{sat} and A_{sat} correlating was recovered [30,32]. Our model also targets predictive outcomes differing from recent optimisation models that aim to predict stomatal responses to leaf water potential, given a carbon cost of losing hydraulic supply [1,22]. Instead, our model prescribes the relative shape of the stomatal response to water potential and effectively assigns carbon costs to the slope and intercept of this function. Our optimisation model is much more akin to the model of Buckley and Roberts [26] in that it allocates carbon to different traits and performs the optimisation in terms of those traits, but at the leaf level only and considers time-averaged properties, not growth.

By focussing on long-term adaptive traits, our model cannot predict the short-term dynamic responses of stomata to the environment. However, our model has allowed the estimation of the relative costs of leaf traits fundamental to maintaining gas

exchange for photosynthesis by building the model in terms of these traits. In capturing fundamental relations between leaf photosynthesis, gas exchange and water relations, our model provides a basis for predicting the long-term adaption of traits to the environment.

Methods

Leaf carbon balance and the representation of costs

The optimisation model is based on a carbon income-cost approach, with the aim of maximising the rate of net carbon gain of a leaf per leaf area (C_{gain}). The carbon income to the plant is taken to be the time-averaged CO_2 assimilation rate per leaf area over a sufficiently long timescale to encompass a number of cycles of leaf replacement, while the individual carbon costs per leaf area (both building and maintenance) for component traits supporting CO_2 assimilation are taken as expenses. The aim is to be able to solve for leaf traits given species variation in A_{sat}, which is somewhat akin to taking the photosynthetic nitrogen investment per leaf area of a species as the known variation. Because the optimisation is aimed at explaining long-term traits, the time averaged CO_2 assimilation rate is expressed in terms of A_{sat}, multiplied by an effective fraction of time (f) that CO_2 assimilation was at A_{sat}. That is, the mean rate of carbon gain is

$$C_{\text{gain}} = A_{\text{sat}} f - costs, \quad (1)$$

such that

$$f = \frac{\int_{t_1}^{t_2} A(t)\mathrm{d}t}{\int_{t_1}^{t_2} A_{\text{sat}}\mathrm{d}t}, \quad (2)$$

where $A(t)$ is the CO_2 assimilation rate per leaf area at time t and t_1 and t_2 represent bounds on some large time interval of active leaf function. A_{sat} is assumed constant for an individual under a particular environment, not dynamically changing under a dynamic environment.

The gain of carbon in the optimisation is expressed in terms of a net rate of CO_2 uptake per leaf area. This requires the carbon cost of traits to be also expressed as a rate of CO_2 loss per leaf area. It is important to consider what these costs encompass. Here the carbon cost of a physiological trait can be broadly partitioned into three components: a once-off cost to build the trait, a continual background maintenance cost for the trait, and a maintenance cost for the trait that is higher when the plant is photosynthesising in the light. These costs should be approximately proportional to some function of the particular trait in question. Considering the costs as a rate of carbon loss per leaf area, then the building cost is effectively spread over the mean lifespan of the leaf (τ), while the light-dependent maintenance cost is only operating for approximately f of the time, and the carbon balance is

$$C_{\text{gain}} = A_{\text{sat}} f - \sum_{\text{traits}} \left(\frac{\mu_{\text{b}}}{\tau} + \mu_{\text{mc}} + \mu_{\text{ml}} f \right) h_{\text{trait}}, \quad (3)$$

where μ_{b}, μ_{mc} and μ_{ml} are the proportionality constants for building, continual maintenance and light-dependent maintenance costs, respectively, h_{trait} is the functional dependence of the costs on the trait, and total costs are summed over the physiological traits in question.

In practice, not all of μ_{b}, μ_{mc} and μ_{ml} are known for each trait, nor are f or τ necessarily known for a leaf either. It is best then to group the unknowns into common parameters and do the optimisation not in terms of C_{gain} but $F = C_{\text{gain}}/f$, so that

$$F = A_{\text{sat}} - \sum_{\text{traits}} \frac{1}{f} \left(\frac{\mu_{\text{b}}}{\tau} + \mu_{\text{mc}} + \mu_{\text{ml}} f \right) h_{\text{trait}} = A_{\text{sat}} - \sum_{\text{traits}} \mu_{\text{trait}} h_{\text{trait}}, \quad (4)$$

where μ_{trait} is the constant of proportionality for the cost of a trait, or the cost coefficient for the trait. In this way the unknown f, τ, μ_b, μ_{mc} and μ_{ml} are absorbed into one parameter μ_{trait}, which is used in the model. If any one of the unknown parameters changes between species independently of the other parameters, then the apparent cost coefficient of the trait is also expected to vary between species.

Key to the optimisation is the identification of the important traits, an expression for A_{sat} in terms of these traits and consideration of how the carbon costs of these traits should scale (in terms of a cost to CO_2 assimilation rate).

CO_2 assimilation rate in terms of the key component traits

CO_2 assimilation rate is the key income of carbon for plants. Thus it is important to be able to express A_{sat} physiologically in terms of the key functional traits. A_{sat} was modelled using the linearised form of Rubisco-limited kinetics [8] as

$$A_{\mathrm{sat}} = k(C_{\mathrm{i}} - \Gamma^*), \quad (5)$$

such that

$$k = \frac{V_{\mathrm{cmax}}}{K_{\mathrm{m}} + \Gamma^*} \quad (6)$$

[51], where C_i is the CO_2 concentration inside the leaf, Γ^* is the CO_2 compensation point in the absence of respiration, K_m is the Michaelis-Menten constant for carboxylation at 21% O_2 and V_{cmax} is the maximum rate of carboxylation by Rubisco per leaf area. The linearised form was used for simplicity and has successfully been utilised in a number of optimisation schemes [30,79,80]. However, optimisations using the linear form predict the incorrect responses of g_s to ambient CO_2 [7,28,32]; thus changes to ambient CO_2 were not considered. Respiration rate was not included in the expression for A_{sat}

494 for simplicity and because respiration should form part of the metabolic costs of
495 supporting CO_2 assimilation.
496 Diffusion of CO_2 into the leaf was described using Fick's Law, assuming well-mixed
497 conditions (infinite boundary layer conductance), as
498 $$A_{\mathrm{sat}} = \frac{g_{\mathrm{sat}}}{1.6}(C_{\mathrm{a}} - C_{\mathrm{i}}), \quad (7)$$
499 where C_a is the CO_2 concentration in the ambient air surrounding the leaf, g_{sat} is the
500 light-saturated stomatal conductance to water vapour per leaf area, and the factor 1.6
501 converts conductance to water vapour to conductance to CO_2.
502 Eliminating C_i between equations 5 and 7 gives
503 $$A_{\mathrm{sat}} = \frac{k g_{\mathrm{sat}}(C_{\mathrm{a}} - \Gamma^*)}{1.6k + g_{\mathrm{sat}}}. \quad (8)$$
504 Stomata are turgor-controlled pores; thus it was assumed that g_{sat} behaves as if it is
505 controlled hydraulically in response to changes in leaf water status. g_{sat} was
506 approximated as a linear function of leaf turgor pressure (P)
507 $$g_{\mathrm{sat}} = \chi P, \quad (9)$$
508 where χ is the constant of proportionality [66,81]. This approximation captures the linear
509 increase of stomatal aperture with increasing guard cell turgor pressure at non-
510 saturating turgor pressures [82,83] and the generally observed coordination between
511 stomatal closure and turgor loss point [15]. For stomata of equal size and shape, χ is
512 indicative of stomatal density.
513 Leaf turgor pressure depends on both the leaf osmotic pressure (π) and leaf water
514 potential (Ψ_l) through the equation
515 $$P = \pi + \Psi_{\mathrm{l}}. \quad (10)$$
516 However, π is not constant, but changes because of dilution and concentration of
517 solutes as cell volume changes from hydration and dehydration, respectively. For a

given amount of solute in a cell, changes in osmotic pressure with changes in cell volume can be expressed as

$$\pi = \frac{\pi_{\mathrm{tlp}} V_{\mathrm{tlp}}}{V}, \quad (11)$$

where V is the cell volume and where we have taken the reference as the turgor loss point, such that π_{tlp} and V_{tlp} are the osmotic pressure and cell volume at turgor loss point, respectively.

Changes in cell turgor pressure are related to changes in cell volume while plant cells are turgid by

$$\varepsilon = V \frac{dP}{dV}, \quad (12)$$

where ε is the elastic modulus.

Taking into account the effect that changes in cell volume have on leaf osmotic pressure through dilution, by approximating the derivative of equation 12 by a finite difference around the turgor loss point and then combining with equations 10 and 11, P can be written as

$$P = \frac{\pi_{\mathrm{tlp}} + \Psi_{\mathrm{l}}}{\left(1 + \frac{\pi_{\mathrm{tlp}}}{\varepsilon}\right)}. \quad (13)$$

Eliminating Ψ_{l} requires knowledge of leaf water balance. Liquid (J) and vapour (E) fluxes of water per unit leaf area into and out of the leaf are balanced at steady state. Again assuming well-mixed conditions, the flux balance can be described as

$$J = K_{\mathrm{leaf}} \Delta\Psi = K_{\mathrm{leaf}} (\Psi_{\mathrm{s}} - \Psi_{\mathrm{l}}) = E = g_{\mathrm{sat}} \Delta w, \quad (14)$$

where K_{leaf} is the leaf hydraulic conductance per leaf area, Ψ_{s} is the source water potential (the terminal twig or petiole water potential) and Δw is the leaf-to-air vapour mole fraction difference (leaf-to-air vapour pressure difference divided by atmospheric pressure). Rearranging gives Ψ_{l} as

$$\Psi_{\mathrm{l}} = \Psi_{\mathrm{s}} - \frac{g_{\mathrm{sat}} \Delta w}{K_{\mathrm{leaf}}}. \quad (15)$$

Eliminating Ψ_l from equation 13 using equation 15 and substituting into equation 9 gives g_{sat} as

$$g_{\mathrm{sat}} = \frac{\chi K_{\mathrm{leaf}}(\pi_{\mathrm{tlp}}+\Psi_{\mathrm{s}})}{K_{\mathrm{leaf}}\left(1+\frac{\pi_{\mathrm{tlp}}}{\varepsilon}\right)+\chi\Delta w}. \quad (16)$$

Finally, substituting equation 16 into equation 8 gives

$$A_{\mathrm{sat}} = \frac{k(C_{\mathrm{a}}-\Gamma^{*})\chi K_{\mathrm{leaf}}(\pi_{\mathrm{tlp}}+\Psi_{\mathrm{s}})}{1.6k\left[K_{\mathrm{leaf}}\left(1+\frac{\pi_{\mathrm{tlp}}}{\varepsilon}\right)+\chi\Delta w\right]+\chi K_{\mathrm{leaf}}(\pi_{\mathrm{tlp}}+\Psi_{\mathrm{s}})}. \quad (17)$$

This is an expression for A_{sat} in terms of physical traits to be solved for (χ, K_{leaf} and π_{tlp}), ε and environmental conditions (Δw and Ψ_s).

The carbon costs of stomata, hydraulics and osmotic pressure

Here we consider how the carbon costs of stomata (χ), hydraulics (K_{leaf}) and osmotic pressure at turgor loss point (π_{tlp}) should scale in terms of a cost to CO_2 assimilation rate per leaf area.

Stomata (χ) – If stomatal size and shape remains approximately constant across species so that each individual pore is contributing the same small amount to overall stomatal conductance, then the slope of stomatal conductance to turgor pressure (χ) will increase proportionally with stomatal density. We can then see that χ is indicative of stomatal density. Stomatal density, like A_{sat}, is a surface property, so that the carbon cost of stomata per area should be proportional to the density of stomata, or

$$cost_{\chi} = \mu_{\chi}\chi, \quad (18)$$

where μ_{χ} is the cost parameter for χ.

Hydraulics (K_{leaf}) – How the carbon cost of hydraulics scales with K_{leaf} is less clear, because differences in vessel architecture, leaf venation pattern, vein density and leaf thickness can all influence K_{leaf} [13,48-50]. For simplicity, and to allow comparisons

between single and multiveined species, it was assumed that the carbon cost of hydraulics scaled with K_{leaf}, given that K_{leaf} is a per area quantity, or

$$cost_{\mathrm{K}} = \mu_{\mathrm{K}} K_{\mathrm{leaf}}, \quad (19)$$

where μ_{K} is the cost parameter for K_{leaf}.

Osmotic pressure at turgor loss point (π_{tlp}) – Osmotic pressure inside the cells of a leaf is approximately proportional to the concentration of solutes in the cells [84]. The carbon cost of osmotic pressure in the cell should depend on the amount of solute present, so that the cost is higher when either the concentration of solutes is higher for a given volume, or higher when the volume is greater for the same concentration of solutes. This means that per leaf area, the carbon cost of osmotic pressure depends on both osmotic pressure at turgor loss point and the depth of relevant tissue. To incorporate this depth, we assumed that a leaf increases photosynthetic capacity by increasing the depth of photosynthetic tissue and that V_{cmax} per depth of photosynthetic tissue is somewhat conserved, such as is typically the case for plastic adaptation to growth in shade vs. sun leaves [85]. Note that this depth is different from true leaf thickness, as the latter can represent structural adaptation for leaf longevity [4,72]. The cost of osmotic pressure can be written as

$$cost_{\pi} = \frac{\mu_{\pi}}{v} \pi_{\mathrm{tlp}} k, \quad (20)$$

where μ_{π} is the cost parameter for π_{tlp} and v is the k per depth of photosynthetic tissue, so that k/v is a depth. The more natural cost parameter is μ_{π}/v and it is used throughout.

In practice there is also a carbon cost for ε; however, the cost was ignored because our data sets do not include ε and it was unclear how the cost might be expected to scale.

Combining the assimilation benefit from equation 17 and the carbon costs of the traits of interest from equations 18-20 into equation 4 gives the net carbon gain as

591 $$F = \frac{k(C_a-\Gamma^*)\chi K_{leaf}(\pi_{tlp}+\Psi_s)}{1.6k\left[K_{leaf}\left(1+\frac{\pi_{tlp}}{\varepsilon}\right)+\chi\Delta w\right]+\chi K_{leaf}(\pi_{tlp}+\Psi_s)} - \mu_\chi\chi - \mu_K K_{leaf} - \frac{\mu_\pi}{v}\pi_{tlp}k. \quad (21)$$

592

593 *Solutions and predictions of optimal leaves*

594

595 An optimal leaf maximises net carbon gain, but what values of χ, K_{leaf} and π maximise
596 net carbon gain for a given A_{sat} and environmental conditions? The optimum occurs
597 when

598 $$\nabla F = \underline{0}, \quad (22a)$$

599 or

600 $$\frac{\partial F}{\partial \chi} = \frac{\partial F}{\partial K_{leaf}} = \frac{\partial F}{\partial \pi_{tlp}} = 0. \quad (22b)$$

601 The partial derivatives provide three equations, one for each cost parameter. These
602 can be expressed in terms of A_{sat} after eliminating k using equation 17 as

603 $$\mu_\chi = \frac{1.6\left(1+\frac{\pi_{tlp}}{\varepsilon}\right)}{(C_a-\Gamma^*)(\pi_{tlp}+\Psi_s)\chi^2}A_{sat}^2, \quad (23)$$

604 $$\mu_K = \frac{1.6\Delta w}{(C_a-\Gamma^*)(\pi_{tlp}+\Psi_s)K_{leaf}^2}A_{sat}^2 \quad (24)$$

605 and

606 $$\frac{\mu_\pi}{v} = \frac{1.6\left[K_{leaf}\left(1-\frac{\Psi_s}{\varepsilon}\right)+\chi\Delta w\right]}{k(C_a-\Gamma^*)(\pi_{tlp}+\Psi_s)^2\chi K_{leaf}}A_{sat}^2 =$$

607 $$\frac{1.6\left[K_{leaf}\left(1-\frac{\Psi_s}{\varepsilon}\right)+\chi\Delta w\right]\left\{(C_a-\Gamma^*)\chi K_{leaf}(\pi_{tlp}+\Psi_s)-1.6A_{sat}\left[K_{leaf}\left(1+\frac{\pi_{tlp}}{\varepsilon}\right)+\chi\Delta w\right]\right\}}{(C_a-\Gamma^*)(\pi_{tlp}+\Psi_s)^3\chi^2K_{leaf}^2}A_{sat}. \quad (25)$$

608 These can be solved analytically for the three unknown traits. π_{tlp} is the solution to

609 $$\frac{\left(\frac{\mu_\pi}{v}\right)}{\mu_\chi}\left(1+\frac{\pi_{\mathrm{tlp}}}{\varepsilon}\right)\left(\pi_{\mathrm{tlp}}+\Psi_{\mathrm{s}}\right)^2-\left\{\left(1-\frac{\Psi_{\mathrm{s}}}{\varepsilon}\right)+\left[\frac{\mu_{\mathrm{K}}\Delta w}{\mu_\chi}\left(1+\right.\right.\right.$$

610 $$\left.\left.\left.\frac{\pi_{\mathrm{tlp}}}{\varepsilon}\right)\right]^{\frac{1}{2}}\right\}\left\{\left[\frac{1.6\left(1+\frac{\pi_{\mathrm{tlp}}}{\varepsilon}\right)(C_{\mathrm{a}}-\Gamma^*)(\pi_{\mathrm{tlp}}+\Psi_{\mathrm{s}})}{\mu_\chi}\right]^{\frac{1}{2}}-1.6\left[\left(1+\frac{\pi_{\mathrm{tlp}}}{\varepsilon}\right)+\left[\frac{\mu_{\mathrm{K}}\Delta w}{\mu_\chi}\left(1+\frac{\pi_{\mathrm{tlp}}}{\varepsilon}\right)\right]^{\frac{1}{2}}\right]\right\}=0.$$

611 (26)

612 This has to be solved numerically, but importantly π_{tlp} is independent of A_{sat}, and

613 conserved under the same environmental conditions and cost parameters.

614 Other traits can be solved once optimal osmotic pressure is known. The solutions to

615 the other two traits are

616 $$\chi=\left[\frac{1.6\left(1+\frac{\pi_{\mathrm{tlp}}}{\varepsilon}\right)}{\mu_\chi(C_{\mathrm{a}}-\Gamma^*)(\pi_{\mathrm{tlp}}+\Psi_{\mathrm{s}})}\right]^{\frac{1}{2}}A_{\mathrm{sat}} \quad (27)$$

617 and

618 $$K_{\mathrm{leaf}}=\left[\frac{1.6\Delta w}{\mu_{\mathrm{K}}(C_{\mathrm{a}}-\Gamma^*)(\pi+\Psi_{\mathrm{s}})}\right]^{\frac{1}{2}}A_{\mathrm{sat}}. \quad (28)$$

619 That is, both χ and K_{leaf} are proportional to A_{sat} in optimal leaves under the same

620 environmental conditions, ε and constant cost parameters.

621 The χ vs. A_{sat} relation is more intuitive when expressed as a g_{sat} vs. A_{sat} relation. The

622 g_{sat} vs. A_{sat} relation can be obtained from equations 16, 27 and 28 as

623 $$g_{\mathrm{sat}}=\frac{\left[\frac{1.6\left(\pi_{\mathrm{tlp}}+\Psi_{\mathrm{s}}\right)}{\mu_\chi(C_{\mathrm{a}}-\Gamma^*)\left(1+\frac{\pi_{\mathrm{tlp}}}{\varepsilon}\right)}\right]^{\frac{1}{2}}}{1+\left[\frac{\mu_{\mathrm{K}}\Delta w}{\mu_\chi\left(1+\frac{\pi_{\mathrm{tlp}}}{\varepsilon}\right)}\right]^{\frac{1}{2}}}A_{\mathrm{sat}}. \quad (29)$$

624 Equation 29 gives the usual optimisation result of g_{sat} being proportional to A_{sat} [30,32].

625 Equations 28 and 29 show that $g_{\mathrm{sat}}/K_{\mathrm{leaf}}$ is constant for constant cost parameters and

626 environmental conditions. Substituting into equation 15 gives

$$\Delta\Psi = \Psi_s - \Psi_l = \frac{(\pi_{tlp}+\Psi_s)}{\left[\frac{\mu_\chi\left(1+\frac{\pi_{tlp}}{\varepsilon}\right)}{\mu_K \Delta w}\right]^{\frac{1}{2}}+1}. \quad (30)$$

That is, stem to leaf water potential difference is independent of A_{sat} and conserved in plants possessing the same cost structure, adapted under the same environmental conditions and measured under saturating light conditions.

The optimisation model provides an estimate for the relative cost of each component trait, defined as the percentage each trait contributes to the total cost of building and maintaining stomata, hydraulics and osmotic pressure. The relative costs of stomata (p_χ), hydraulics (p_K) and osmotic pressure (p_π) are

$$p_\chi = \frac{K_{leaf}(\pi_{tlp}+\Psi_s)}{\pi_{tlp}\left\{K_{leaf}\left[1+\frac{\left(1-\frac{\Psi_s}{\varepsilon}\right)}{\left(1+\frac{\pi_{tlp}}{\varepsilon}\right)}\right]+\frac{2\chi\Delta w}{\left(1+\frac{\pi_{tlp}}{\varepsilon}\right)}\right\}+\Psi_s\left\{K_{leaf}+\frac{\chi\Delta w}{\left(1+\frac{\pi_{tlp}}{\varepsilon}\right)}\right\}}, \quad (31)$$

$$p_K = \frac{\frac{\chi\Delta w}{\left(1+\frac{\pi_{tlp}}{\varepsilon}\right)}(\pi_{tlp}+\Psi_s)}{\pi_{tlp}\left\{K_{leaf}\left[1+\frac{\left(1-\frac{\Psi_s}{\varepsilon}\right)}{\left(1+\frac{\pi_{tlp}}{\varepsilon}\right)}\right]+\frac{2\chi\Delta w}{\left(1+\frac{\pi_{tlp}}{\varepsilon}\right)}\right\}+\Psi_s\left\{K_{leaf}+\frac{\chi\Delta w}{\left(1+\frac{\pi_{tlp}}{\varepsilon}\right)}\right\}} \quad (32)$$

and

$$p_\pi = \frac{1}{\left(1+\frac{\Psi_s}{\pi_{tlp}}\right)\left[\frac{K_{leaf}\left(1+\frac{\pi_{tlp}}{\varepsilon}\right)+\chi\Delta w}{K_{leaf}\left(1-\frac{\Psi_s}{\varepsilon}\right)+\chi\Delta w}\right]+1}. \quad (33)$$

A full derivation of the model is presented in the Supplementary Methods.

Model testing

The optimisation model was tested on data from 41 species encompassing lycophytes, ferns, gymnosperms and angiosperms and a range of adaptive conditions from Brodribb, et al. [13]. Each species was treated as a distinct sample. Of these, 16 species had a complete set of A_{sat}, g_{sat}, K_{leaf} and π_{tlp} (originally from Brodribb and Holbrook

[86]), while the remaining species possessed data for A_{sat}, g_{sat} and K_{leaf} only (Supplementary Table 1). The former set of 16 species was used to fit the model by solving for the unknown cost parameters, while the model was tested on both this set and the full set of 41 species. The aim was to determine whether the model could explain observed trends across species in osmotic pressure, stomatal conductance and leaf hydraulic conductance, as well as estimate relative costs of stomata, hydraulics and osmotic pressure.

The optimisation model was first fitted to data from the 16 species that possessed a complete set of A_{sat}, g_{sat}, K_{leaf} and π_{tlp} for each species. This was done by calculating cost parameters for stomata (μ_χ, equation 23), hydraulics (μ_K, equation 24) and osmotic pressure (μ_π/v, equation 25) using A_{sat}, g_{sat}, K_{leaf} and π_{tlp} for each species, and assuming an ε of 10 MPa and Γ^* of 48.4 μmol mol^{-1} at 25 °C [87]. C_a was 400 μmol mol^{-1}, while Δw was set at 0.015, the midrange of Δw during measurement. Well-watered conditions (Ψ_s = 0 MPa) were also assumed. In all cases g_{sat} for each species was first converted to χ using

$$\chi = \frac{g_{sat}\left(1+\frac{\pi_{tlp}}{\varepsilon}\right)}{(\pi_{tlp}+\Psi_s)-\frac{g_{sat}\Delta w}{K_{leaf}}} \quad (34)$$

(obtained from rearranging equation 12).

The across-species means of the cost parameters for stomata, hydraulics and osmotic pressure were taken as the best estimates for each cost parameter. Cost parameter estimates were (mean ± s.e.): μ_χ = 16.9 ± 4.0 μmol mol^{-1} MPa, μ_K = 44.1 ± 5.5 μmol mol^{-1} MPa and μ_π/v = 31.0 ± 3.1 μmol mol^{-1} MPa^{-1}. These cost parameters were then used as inputs to first calculate optimal π_{tlp} by numerically solving equation 26, again assuming ε = 10 MPa, Γ^* = 48.4 μmol mol^{-1}, C_a = 400 μmol mol^{-1}, Δw = 0.015 and Ψ_s = 0 MPa. Optimal $\Delta\Psi$ was also calculated using equation 30. Predicted π_{tlp} was then

used to solve for optimal χ (equation 27), K_{leaf} (equation 28) and g_{sat} (equation 16) for the given A_{sat} of each species, assuming the same values as above for ε, Γ^*, C_a, Δw and Ψ_s. The model-data comparison was made for both the 16 species with full data and the complete 41 species. Model predictions for relations between g_{sat}, K_{leaf} and A_{sat} were compared by R^2. Trends of π_{tlp} and $\Delta\Psi$ against A_{sat} in observed data were tested by linear correlation, and if no significant difference was found then the data were compared against the model prediction by a one-sample *t*-test.

The effects of varying the environmental parameters Δw and Ψ_s on long-term adaptive π_{tlp}, g_{sat} and A_{sat} were modelled using the across-species mean of cost parameters above. ε was assumed to be 10 MPa, Γ^* was 48.4 μmol mol^{-1} and C_a was 400 μmol mol^{-1}. π_{tlp} under different conditions was solved numerically from equation 26. Optimal $\Delta\Psi$ was then calculated using equation 30. Both g_{sat} and A_{sat} were calculated for a constant k, set at the value expected for an optimal leaf at a reference A_{sat} of 15 μmol m^{-2} s^{-1} at a Ψ_s of 0 MPa and Δw of 0.015, using

$$k = \frac{\chi K_{leaf}(\pi_{tlp}+\Psi_s)A_{sat}}{(C_a-\Gamma^*)\chi K_{leaf}(\pi_{tlp}+\Psi_s)-1.6A_{sat}\left[K_{leaf}\left(1+\frac{\pi_{tlp}}{\varepsilon}\right)+\chi\Delta w\right]}, \quad (35)$$

where optimal π_{tlp}, χ and K_{leaf} were calculated from equations 26, 27 and 28, respectively. It can be seen from equation 35 that k and A_{sat} are proportional to each other under constant environmental conditions, because both optimal χ and K_{leaf} are proportional to A_{sat} (equations 27 and 28). Here simulations were done for constant k rather than constant A_{sat} because k is the true source of variation in biochemical photosynthetic capacity and as such is not strictly influenced by Δw or Ψ_s in the model, while A_{sat} depends on g_{sat} and so does depend on Δw and Ψ_s (Fig. 1). Optimal χ and K_{leaf} for different environmental parameters were then calculated as

$$\chi = k\frac{1.6\left(1+\frac{\pi_{tlp}}{\varepsilon}\right)}{(\pi_{tlp}+\Psi_s)}\left\{\left[\frac{(C_a-\Gamma^*)(\pi_{tlp}+\Psi_s)}{1.6\mu_\chi\left(1+\frac{\pi_{tlp}}{\varepsilon}\right)}\right]^{\frac{1}{2}}-\left[1+\left[\frac{\mu_K\Delta w}{\mu_\chi\left(1+\frac{\pi_{tlp}}{\varepsilon}\right)}\right]^{\frac{1}{2}}\right]\right\} \quad (36)$$

and

$$K_{\mathrm{leaf}} = k\frac{1.6}{(\pi_{\mathrm{tlp}}+\Psi_{\mathrm{s}})}\left[\frac{\mu_\chi \Delta w\left(1+\frac{\pi_{\mathrm{tlp}}}{\varepsilon}\right)}{\mu_{\mathrm{K}}}\right]^{\frac{1}{2}}\left\{\left[\frac{(C_{\mathrm{a}}-\Gamma^*)(\pi_{\mathrm{tlp}}+\Psi_{\mathrm{s}})}{1.6\mu_\chi\left(1+\frac{\pi_{\mathrm{tlp}}}{\varepsilon}\right)}\right]^{\frac{1}{2}}-\left[1+\left[\frac{\mu_{\mathrm{K}}\Delta w}{\mu_\chi\left(1+\frac{\pi_{\mathrm{tlp}}}{\varepsilon}\right)}\right]^{\frac{1}{2}}\right]\right\}. \quad (37)$$

g_{sat} was then calculated using equation 16 and A_{sat} from equation 17. Simulations were carried out for a Δw range of 0.001 to 0.03 at a Ψ_{s} of 0 MPa, and a Ψ_{s} range of 0 to -2 MPa at a Δw of 0.015.

The predictions for how optimal A_{sat} and g_{sat} varied with Δw were compared with that from the linearised Cowan-Farquhar optimisation. The marginal cost of transpiration (μ_{E}) for each species was calculated from the data as

$$\mu_{\mathrm{E}} = \frac{1.6}{\Delta w(C_{\mathrm{a}}-\Gamma^*)g_{\mathrm{sat}}^2}A_{\mathrm{sat}}^2, \quad (38)$$

assuming C_{a} of 400 μmol mol^{-1}, Γ^* of 48.4 μmol mol^{-1} and Δw of 0.015. The mean μ_{E} was then used to simulate the effect of varying Δw on g_{sat} and A_{sat} for constant k, set as that expected for a reference A_{sat} of 15 μmol m^{-2} s^{-1} and Δw of 0.015, using

$$k = \frac{g_{\mathrm{sat}}A_{\mathrm{sat}}}{g_{\mathrm{sat}}(C_{\mathrm{a}}-\Gamma^*)-1.6A_{\mathrm{sat}}}, \quad (39)$$

where optimal g_{sat} for the reference condition was calculated using

$$g_{\mathrm{sat}} = \left[\frac{1.6}{\mu_{\mathrm{E}}\Delta w(C_{\mathrm{a}}-\Gamma^*)}\right]^{\frac{1}{2}}A_{\mathrm{sat}}. \quad (40)$$

Optimal g_{sat} for varying Δw was then calculated using

$$g_{\mathrm{sat}} = 1.6k\left\{\left[\frac{(C_{\mathrm{a}}-\Gamma^*)}{1.6\mu_{\mathrm{E}}\Delta w}\right]^{\frac{1}{2}}-1\right\} \quad (41)$$

and A_{sat} was further calculated using equation 8.

The relative costs of stomata, hydraulics and osmotic pressure were also estimated for each of the 16 species that had measured values for g_{s}, K_{leaf} and π_{tlp}. First χ was again calculated for each species from g_{s}, K_{leaf} and π_{tlp} using equation 34. The relative costs

of stomata, hydraulics and osmotic pressure for each species were then calculated from equations 31, 32 and 33, respectively, from the χ, K_{leaf} and π_{tlp} measured for each species. Other parameters again assumed were: ε = 10 MPa, Γ^* = 48.4 μmol mol^{-1}, C_a = 400 μmol mol^{-1}, Δw = 0.015 and Ψ_s = 0 MPa. Relative costs among physiological traits were compared by a Kruskal-Wallis test with two-sided multiple comparison testing.

All calculations and analyses were performed in MATLAB (Mathworks, Natick, MA, USA).

Data availability statement

Data used are available in Supplementary Table 1. Data and code are available at https://github.com/rossdeans/Deans-et-al.-2020.

Correspondence and requests for materials should be made to G.D.F.

Acknowledgements

We thank Peter Franks for discussions on the coordination of photosynthesis, stomata and leaf hydraulics, Tom Buckley and Roddy Dewar for early discussions on optimisation, and Oliver Binks for general discussions. This work was supported by the Australian Research Council Centre of Excellence for Translational Photosynthesis (CE1401000015). R.M.D. was supported by an ANU Gwendolyn Woodroofe PhD Scholarship.

743

744

745 Author contributions

746

747 R.M.D., T.J.B. and G.D.F. conceived the study. R.M.D. developed the model with

748 input from T.J.B., F.A.B. and G.D.F. T.J.B. provided data. R.M.D. wrote the

749 manuscript with input from T.J.B., F.A.B. and G.D.F.

750

751 Figure legends

752

753 Figure 1. The optimisation scheme for predicting long-term coordination of leaf
754 photosynthetic, gas exchange and water relations traits. Carbon input for a leaf is the
755 light-saturated CO_2 assimilation rate (A_{sat}), which is dependent on leaf biochemical
756 photosynthetic capacity (k) and light-saturated stomatal conductance (g_{sat}). However,
757 for a leaf to obtain a certain g_{sat} requires the appropriate investments in stomata, leaf
758 hydraulics and osmotic pressure, which entails a carbon cost proportional to the trait.
759 Light-saturated stomatal conductance is also dependent on atmospheric evaporative
760 demand (Δw) and petiole source water potential (Ψ_s). The model optimally allocates
761 carbon to the three traits that maximises carbon gain (C_{gain}), the difference between
762 A_{sat} and the carbon costs. Black arrows indicate flows of carbon, while grey arrows
763 indicate leaf physiological links.

764

765

766 Figure 2. Observed and predicted dependence of (a) light-saturated stomatal
767 conductance to the diffusion of water vapour (g_{sat}), (b) leaf hydraulic conductance
768 (K_{leaf}), (c) stem to leaf water potential difference ($\Delta\Psi$) and (d) leaf osmotic pressure at
769 turgor loss point (π_{tlp}) on light-saturated CO_2 assimilation rate (A_{sat}) across species.
770 Black circles represent species for which the full set of A_{sat}, g_{sat}, K_{leaf} and π_{tlp} were
771 known and used for fitting the model, while red circles represent species missing π_{tlp}.
772 Dashed lines represent predicted model trends. The solid line represents the linear line
773 of best fit and dotted lines encompass the 95% confidence interval of the fit. Predicted
774 line in (a) is identical to that from the Cowan-Farquhar model.

775

Figure 3. Long-term adaptive light-saturated CO_2 assimilation rate (A_{sat}), stomatal conductance (g_{sat}), leaf hydraulic conductance (K_{leaf}), osmotic pressure at turgor loss point (π_{tlp}) and stem to leaf water potential difference ($\Delta\Psi$) predicted for a range of leaf to air water mole fraction differences (Δw) and source water potentials (Ψ_s). All model predictions used a photosynthetic capacity expected for a plant with an A_{sat} of 15 μmol m^{-2} s^{-1} at a Δw of 0.015 and Ψ_s of 0 MPa. In (a) and (c), dotted lines represent the predicted Δw dependence for A_{sat} and g_{sat}, respectively, using the linearised Cowan-Farquhar stomatal optimisation model.

Figure 4. Proportion of the total cost of stomata, hydraulics and osmotic pressure attributable to each trait. Centre lines represent medians, boxes cover the 25th and 75th percentile, whiskers cover extremal points not considered outliers, red crosses represent outliers. Black circles represent the mean and error bars are the standard error of the mean. Letters signify significantly different groups from a Kruskal-Wallis test with two-sided multiple comparison testing (n = 16 species; hydraulics-stomata: P = 4.5 x 10^{-4}, hydraulics-osmotic pressure: P = 1.1 x 10^{-8}, stomata-osmotic pressure: n.s.).

797 References

798

799 1 Wolf, A., Anderegg, W. R. & Pacala, S. W. Optimal stomatal behavior with
800 competition for water and risk of hydraulic impairment. *Proceedings of the*
801 *National Academy of Sciences* **113**, E7222-E7230 (2016).
802 2 Cowan, I. R. & Farquhar, G. D. in *Symposia of the Society for Experimental*
803 *Biology.* (ed D.H. Jennings) 471-505.
804 3 Givnish, T. J. in *On the economy of plant form and function: proceedings of*
805 *the Sixth Maria Moors Cabot Symposium, Evolutionary Constraints on*
806 *Primary Productivity, Adaptive Patterns of Energy Capture in Plants,*
807 *Harvard Forest, August 1983.* (Cambridge [Cambridgeshire]: Cambridge
808 University Press, c1986.).
809 4 Wright, I. J. *et al.* The worldwide leaf economics spectrum. *Nature* **428**, 821
810 (2004).
811 5 Körner, C. Maximum leaf diffusive conductance in vascular plants.
812 *Photosynthetica* **13**, 45-82 (1979).
813 6 Wong, S. C., Cowan, I. R. & Farquhar, G. D. Stomatal conductance correlates
814 with photosynthetic capacity. *Nature* **282**, 424-426 (1979).
815 7 Farquhar, G. D. A study of the responses of stomata to perturbations of
816 environment. (1973).
817 8 Cowan, I. in *Advances in botanical research* Vol. 4 117-228 (Elsevier,
818 1978).
819 9 Givnish, T. J. & Vermeij, G. J. Sizes and shapes of liane leaves. *The American*
820 *Naturalist* **110**, 743-778 (1976).
821 10 Brodribb, T. J. Xylem hydraulic physiology: the functional backbone of
822 terrestrial plant productivity. *Plant Science* **177**, 245-251,
823 doi:10.1016/j.plantsci.2009.06.001 (2009).
824 11 Sack, L. & Holbrook, N. M. Leaf hydraulics. *Annu. Rev. Plant Biol.* **57**, 361-
825 381 (2006).
826 12 Brodribb, T. J., Holbrook, N. M., Zwieniecki, M. A. & Palma, B. Leaf
827 hydraulic capacity in ferns, conifers and angiosperms: impacts on
828 photosynthetic maxima. *New phytologist* **165**, 839-846 (2005).
829 13 Brodribb, T. J., Feild, T. S. & Jordan, G. J. Leaf maximum photosynthetic rate
830 and venation are linked by hydraulics. *Plant Physiology* **144**, 1890-1898,
831 doi:10.1104/pp.107.101352 (2007).
832 14 Franks, P. J. Higher rates of leaf gas exchange are associated with higher leaf
833 hydrodynamic pressure gradients. *Plant, Cell & Environment* **29**, 584-592
834 (2006).
835 15 Brodribb, T. J. & Holbrook, N. M. Stomatal closure during leaf dehydration,
836 correlation with other leaf physiological traits. *Plant Physiology* **132**, 2166-
837 2173 (2003).
838 16 Brodribb, T. J. & McAdam, S. A. Evolution of the stomatal regulation of plant
839 water content. *Plant physiology*, pp. 00078.02017 (2017).
840 17 Choat, B. *et al.* Global convergence in the vulnerability of forests to drought.
841 *Nature* **491**, 752 (2012).
842 18 Dewar, R. *et al.* New insights into the covariation of stomatal, mesophyll and
843 hydraulic conductances from optimization models incorporating nonstomatal

limitations to photosynthesis. *New Phytologist* **217**, 571-585, doi:doi:10.1111/nph.14848 (2018).
19 Prentice, I. C., Dong, N., Gleason, S. M., Maire, V. & Wright, I. J. Balancing the costs of carbon gain and water transport: testing a new theoretical framework for plant functional ecology. *Ecology Letters* **17**, 82-91, doi:10.1111/ele.12211 (2014).
20 Huang, C.-W. *et al.* Transport in a coordinated soil-root-xylem-phloem leaf system. *Advances in water resources* **119**, 1-16 (2018).
21 Mrad, A. *et al.* A dynamic optimality principle for water use strategies explains isohydric to anisohydric plant responses to drought. *Frontiers in Forests and Global Change* **2**, 49 (2019).
22 Sperry, J. S. *et al.* Predicting stomatal responses to the environment from the optimization of photosynthetic gain and hydraulic cost. *Plant, cell & environment* **40**, 816-830 (2017).
23 Wang, Y., Sperry, J. S., Anderegg, W. R., Venturas, M. D. & Trugman, A. T. A theoretical and empirical assessment of stomatal optimization modeling. *New Phytologist* (2020).
24 HÖLTTÄ, T., Mencuccini, M. & Nikinmaa, E. A carbon cost–gain model explains the observed patterns of xylem safety and efficiency. *Plant, Cell & Environment* **34**, 1819-1834 (2011).
25 Manzoni, S., Vico, G., Katul, G., Palmroth, S. & Porporato, A. Optimal plant water-use strategies under stochastic rainfall. *Water Resources Research* **50**, 5379-5394 (2014).
26 Buckley, T. N. & Roberts, D. W. DESPOT, a process-based tree growth model that allocates carbon to maximize carbon gain. *Tree Physiology* **26**, 129-144, doi:10.1093/treephys/26.2.129 (2006).
27 Buckley, T. N. & Roberts, D. W. How should leaf area, sapwood area and stomatal conductance vary with tree height to maximize growth? *Tree Physiology* **26**, 145-157, doi:10.1093/treephys/26.2.145 (2006).
28 Buckley, T. N., Sack, L. & Farquhar, G. D. Optimal plant water economy. *Plant, Cell & Environment* **40**, 881-896 (2017).
29 Mencuccini, M. The ecological significance of long-distance water transport: short-term regulation, long-term acclimation and the hydraulic costs of stature across plant life forms. *Plant, Cell & Environment* **26**, 163-182 (2003).
30 Lloyd, J. *et al.* A simple calibrated model of Amazon rainforest productivity based on leaf biochemical properties. *Plant, Cell & Environment* **18**, 1129-1145 (1995).
31 Leuning, R. A critical appraisal of a combined stomatal-photosynthesis model for C3 plants. *Plant, Cell & Environment* **18**, 339-355 (1995).
32 Medlyn, B. E. *et al.* Reconciling the optimal and empirical approaches to modelling stomatal conductance. *Global Change Biology* **17**, 2134-2144, doi:10.1111/j.1365-2486.2010.02375.x (2011).
33 Scoffoni, C. *et al.* Outside-xylem vulnerability, not xylem embolism, controls leaf hydraulic decline during dehydration. *Plant physiology* **173**, 1197-1210 (2017).
34 Scoffoni, C. *et al.* The causes of leaf hydraulic vulnerability and its influence on gas exchange in *Arabidopsis thaliana*. *Plant physiology* **178**, 1584-1601 (2018).
35 Scoffoni, C., McKown, A. D., Rawls, M. & Sack, L. Dynamics of leaf hydraulic conductance with water status: quantification and analysis of species

894 differences under steady state. *Journal of Experimental Botany* **63**, 643-658
895 (2012).
896 36 Brodribb, T. J. *et al.* Visual quantification of embolism reveals leaf
897 vulnerability to hydraulic failure. *New Phytol* **209**, 1403-1409,
898 doi:10.1111/nph.13846 (2016).
899 37 Brodribb, T. J., McAdam, S. A., Jordan, G. J. & Martins, S. C. Conifer species
900 adapt to low-rainfall climates by following one of two divergent pathways.
901 *Proc Natl Acad Sci U S A* **111**, 14489-14493, doi:10.1073/pnas.1407930111
902 (2014).
903 38 Skelton, R. P. *et al.* Low vulnerability to xylem embolism in leaves and stems
904 of North American oaks. *Plant Physiology* **177**, 1066-1077 (2018).
905 39 Skelton, R. P., Brodribb, T. J., McAdam, S. A. & Mitchell, P. J. Gas exchange
906 recovery following natural drought is rapid unless limited by loss of leaf
907 hydraulic conductance: evidence from an evergreen woodland. *New*
908 *Phytologist* **215**, 1399-1412 (2017).
909 40 Passioura, J. B. in *Physiological plant ecology II* 5-33 (Springer, 1982).
910 41 Cardoso, A. A., Brodribb, T. J., Lucani, C. J., DaMatta, F. M. & McAdam, S.
911 A. Coordinated plasticity maintains hydraulic safety in sunflower leaves.
912 *Plant, cell & environment* (2018).
913 42 Farrell, C., Szota, C. & Arndt, S. K. Does the turgor loss point characterize
914 drought response in dryland plants? *Plant, cell & environment* **40**, 1500-1511
915 (2017).
916 43 Brodribb, T. & Feild, T. Stem hydraulic supply is linked to leaf photosynthetic
917 capacity: evidence from New Caledonian and Tasmanian rainforests. *Plant,*
918 *Cell & Environment* **23**, 1381-1388 (2000).
919 44 Franks, P. J. & Farquhar, G. D. A relationship between humidity response,
920 growth form and photosynthetic operating point in C3 plants. *Plant, Cell &*
921 *Environment* **22**, 1337-1349 (1999).
922 45 de Boer, H. J. *et al.* Optimal allocation of leaf epidermal area for gas
923 exchange. *New Phytol* **210**, 1219-1228, doi:10.1111/nph.13929 (2016).
924 46 Franks, P. J. & Beerling, D. J. Maximum leaf conductance driven by CO2
925 effects on stomatal size and density over geologic time. *Proc. Natl. Acad. Sci.*
926 *U. S. A.* **106**, 10343-10347, doi:10.1073/pnas.0904209106 (2009).
927 47 Raven, J. A. Speedy small stomata? *Journal of Experimental Botany* **65**, 1415-
928 1424, doi:10.1093/jxb/eru032 (2014).
929 48 Feild, T. S. & Brodribb, T. J. Hydraulic tuning of vein cell microstructure in
930 the evolution of angiosperm venation networks. *New Phytologist* **199**, 720-726
931 (2013).
932 49 Rockwell, F. E. & Holbrook, N. M. Leaf hydraulic architecture and stomatal
933 conductance: a functional perspective. *Plant Physiology* **174**, 1996-2007,
934 doi:10.1104/pp.17.00303 (2017).
935 50 Sack, L., Scoffoni, C., Johnson, D. M., Buckley, T. N. & Brodribb, T. J. The
936 Anatomical Determinants of Leaf Hydraulic Function. 255-271,
937 doi:10.1007/978-3-319-15783-2_10 (2015).
938 51 Farquhar, G. D., von Caemmerer, S. & Berry, J. A. A biochemical model of
939 photosynthetic CO2 assimilation in leaves of C3 species. *Planta* **149**, 78-90
940 (1980).
941 52 Arneth, A. *et al.* Response of central Siberian Scots pine to soil water deficit
942 and long-term trends in atmospheric CO_2 concentration. *Global*
943 *Biogeochemical Cycles* **16**, 5-1-5-13, doi:10.1029/2000gb001374 (2002).

53 Farquhar, G. D. Models of integrated photosynthesis of cells and leaves. *Philosophical Transactions of the Royal Society of London. B, Biological Sciences* **323**, 357-367 (1989).
54 Deans, R. M., Farquhar, G. D. & Busch, F. A. Estimating stomatal and biochemical limitations during photosynthetic induction. *Plant, Cell & Environment* **42**, 3227-3240 (2019).
55 de Boer, H. J. *et al.* Apparent overinvestment in leaf venation relaxes leaf morphological constraints on photosynthesis in arid habitats. *Plant physiology* **172**, 2286-2299 (2016).
56 Bartlett, M. K., Scoffoni, C. & Sack, L. The determinants of leaf turgor loss point and prediction of drought tolerance of species and biomes: a global meta-analysis. *Ecology Letters* **15**, 393-405 (2012).
57 Lenz, T. I., Wright, I. J. & Westoby, M. Interrelations among pressure-volume curve traits across species and water availability gradients. *Physiologia Plantarum* **127**, 423-433, doi:10.1111/j.1399-3054.2006.00680.x (2006).
58 Nardini, A. & Luglio, J. Leaf hydraulic capacity and drought vulnerability: possible trade-offs and correlations with climate across three major biomes. *Functional Ecology* **28**, 810-818 (2014).
59 Gleason, S. M. *et al.* Weak tradeoff between xylem safety and xylem-specific hydraulic efficiency across the world's woody plant species. *New Phytologist* **209**, 123-136 (2016).
60 Bartlett, M. K., Klein, T., Jansen, S., Choat, B. & Sack, L. The correlations and sequence of plant stomatal, hydraulic, and wilting responses to drought. *Proceedings of the National Academy of Sciences* **113**, 13098-13103 (2016).
61 Sack, L., Cowan, P., Jaikumar, N. & Holbrook, N. The 'hydrology'of leaves: co-ordination of structure and function in temperate woody species. *Plant, Cell & Environment* **26**, 1343-1356 (2003).
62 West, G. B., Brown, J. H. & Enquist, B. J. A general model for the structure and allometry of plant vascular systems. *Nature* **400**, 664-667 (1999).
63 Skelton, R. P., Brodribb, T. J. & Choat, B. Casting light on xylem vulnerability in an herbaceous species reveals a lack of segmentation. *New Phytologist* **214**, 561-569 (2017).
64 Bouche, P. S. *et al.* Are needles of Pinus pinaster more vulnerable to xylem embolism than branches? New insights from X-ray computed tomography. *Plant, cell & environment* **39**, 860-870 (2016).
65 Creek, D., Blackman, C. J., Brodribb, T. J., Choat, B. & Tissue, D. T. Coordination between leaf, stem, and root hydraulics and gas exchange in three arid-zone angiosperms during severe drought and recovery. *Plant, Cell & Environment* **41**, 2869-2881 (2018).
66 Buckley, T., Mott, K. & Farquhar, G. A hydromechanical and biochemical model of stomatal conductance. *Plant, Cell & Environment* **26**, 1767-1785 (2003).
67 Dewar, R. Interpretation of an empirical model for stomatal conductance in terms of guard cell function. *Plant, Cell & Environment* **18**, 365-372 (1995).
68 Murray, M. *et al.* Convergence in maximum stomatal conductance of c3 woody angiosperms in natural ecosystems across bioclimatic zones. *Frontiers in plant science* **10**, 558 (2019).
69 Cowan, I. in *Physiological plant ecology II* 589-613 (Springer, 1982).

70 Bartlett, M. K., Detto, M. & Pacala, S. W. Predicting shifts in the functional composition of tropical forests under increased drought and CO 2 from trade-offs among plant hydraulic traits. *Ecology letters* **22**, 67-77 (2019).
71 Lu, Y., Duursma, R. A., Farrior, C. E., Medlyn, B. E. & Feng, X. Optimal stomatal drought response shaped by competition for water and hydraulic risk can explain plant trait covariation. *New Phytologist* **225**, 1206-1217 (2020).
72 Osnas, J. L. *et al.* Divergent drivers of leaf trait variation within species, among species, and among functional groups. *Proceedings of the National Academy of Sciences* **115**, 5480-5485 (2018).
73 de Vries, F. W. T. P. The Cost of Maintenance Processes in Plant Cells. *Annals of Botany* **39**, 77-92, doi:10.1093/oxfordjournals.aob.a084919 (1975).
74 Hills, A., Chen, Z. H., Amtmann, A., Blatt, M. R. & Lew, V. L. OnGuard, a computational platform for quantitative kinetic modeling of guard cell physiology. *Plant Physiol* **159**, 1026-1042, doi:10.1104/pp.112.197244 (2012).
75 John, G. P. *et al.* The anatomical and compositional basis of leaf mass per area. *Ecology Letters* **20**, 412-425, doi:10.1111/ele.12739 (2017).
76 Navas, M. L. *et al.* Leaf life span, dynamics and construction cost of species from Mediterranean old-fields differing in successional status. *New phytologist* **159**, 213-228 (2003).
77 Vico, G., Manzoni, S., Palmroth, S. & Katul, G. Effects of stomatal delays on the economics of leaf gas exchange under intermittent light regimes. *New Phytologist* **192**, 640-652, doi:10.1111/j.1469-8137.2011.03847.x (2011).
78 Assmann, S. M. & Zeiger, E. Guard cell bioenergetics. *Stomatal function*, 163-193 (1987).
79 Lloyd, J. Modelling stomatal responses to environment in Macadamia integrifolia. *Functional Plant Biology* **18**, 649-660 (1991).
80 Hari, P., Mäkelä, A., Korpilahti, E. & Holmberg, M. Optimal control of gas exchange. *Tree physiology* **2**, 169-175 (1986).
81 Deans, R. M., Brodribb, T. J. & McAdam, S. A. An integrated hydraulic-hormonal model of conifer stomata predicts water stress dynamics. *Plant physiology* **174**, 478-486 (2017).
82 Franks, P. J., Cowan, I. R. & Farquhar, G. D. A study of stomatal mechanics using the cell pressure probe. *Plant, Cell & Environment* **21**, 94-100 (1998).
83 Franks, P. J. & Farquhar, G. D. The mechanical diversity of stomata and its significance in gas-exchange control. *Plant Physiology* **143**, 78-87 (2007).
84 Tyree, M. & Hammel, H. The measurement of the turgor pressure and the water relations of plants by the pressure-bomb technique. *Journal of experimental Botany* **23**, 267-282 (1972).
85 Boardman, N. K. Comparative photosynthesis of sun and shade plants. *Annual review of plant physiology* **28**, 355-377 (1977).
86 Brodribb, T. J. & Holbrook, N. M. Declining hydraulic efficiency as transpiring leaves desiccate: two types of response. *Plant Cell Environ* **29**, 2205-2215, doi:10.1111/j.1365-3040.2006.01594.x (2006).
87 Sharwood, R. E., Ghannoum, O., Kapralov, M. V., Gunn, L. H. & Whitney, S. M. Temperature responses of Rubisco from Paniceae grasses provide opportunities for improving C3 photosynthesis. *Nature Plants* **2**, 16186 (2016).

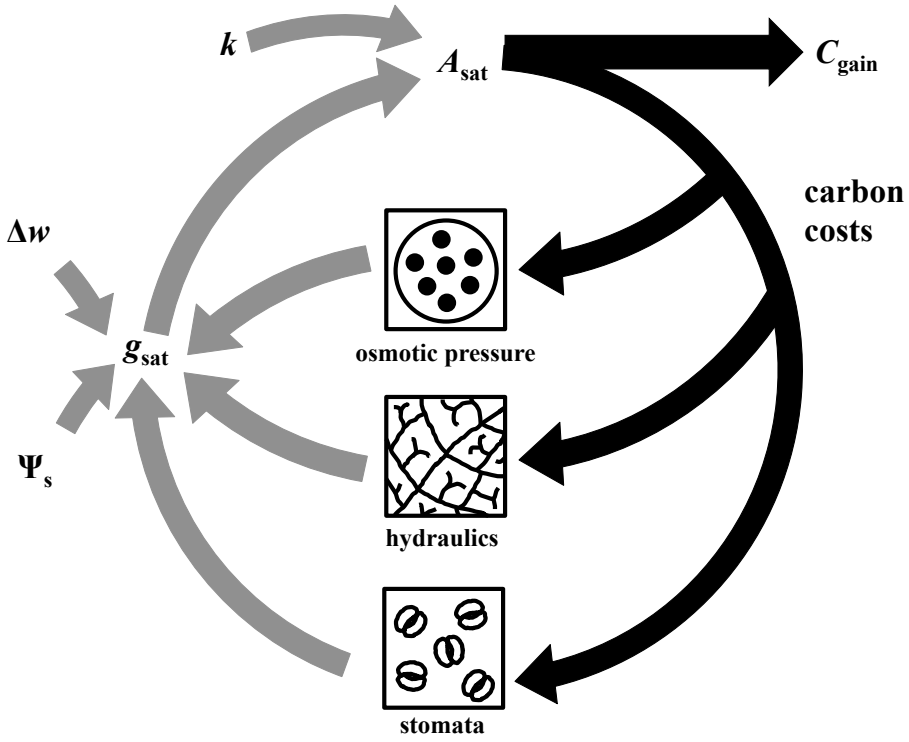
k
A_{sat}
C_{gain}
carbon
costs
Δw
g_{sat}
osmotic pressure
Ψ_s
hydraulics
stomata

1041

1042

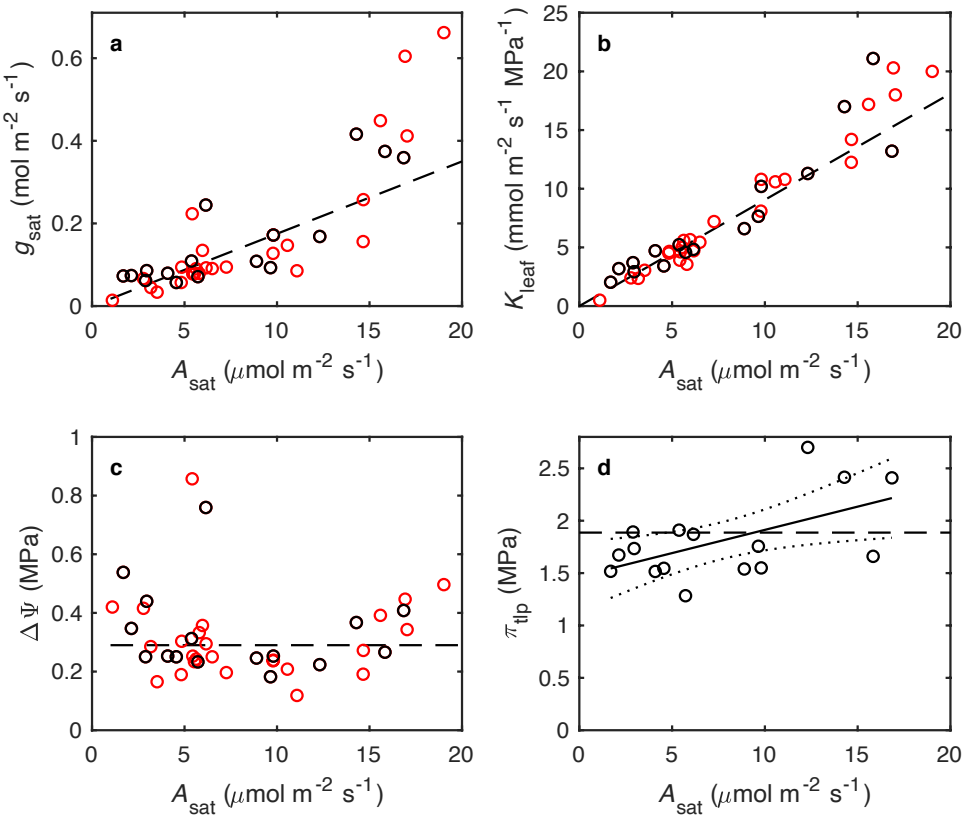
a
b
c
d
g_{sat} (mol m^{-2} s^{-1})
K_{leaf} (mmol m^{-2} s^{-1} MPa^{-1})
$\Delta\Psi$ (MPa)
π_{tlp} (MPa)
A_{sat} (μmol m^{-2} s^{-1})

1043

1044

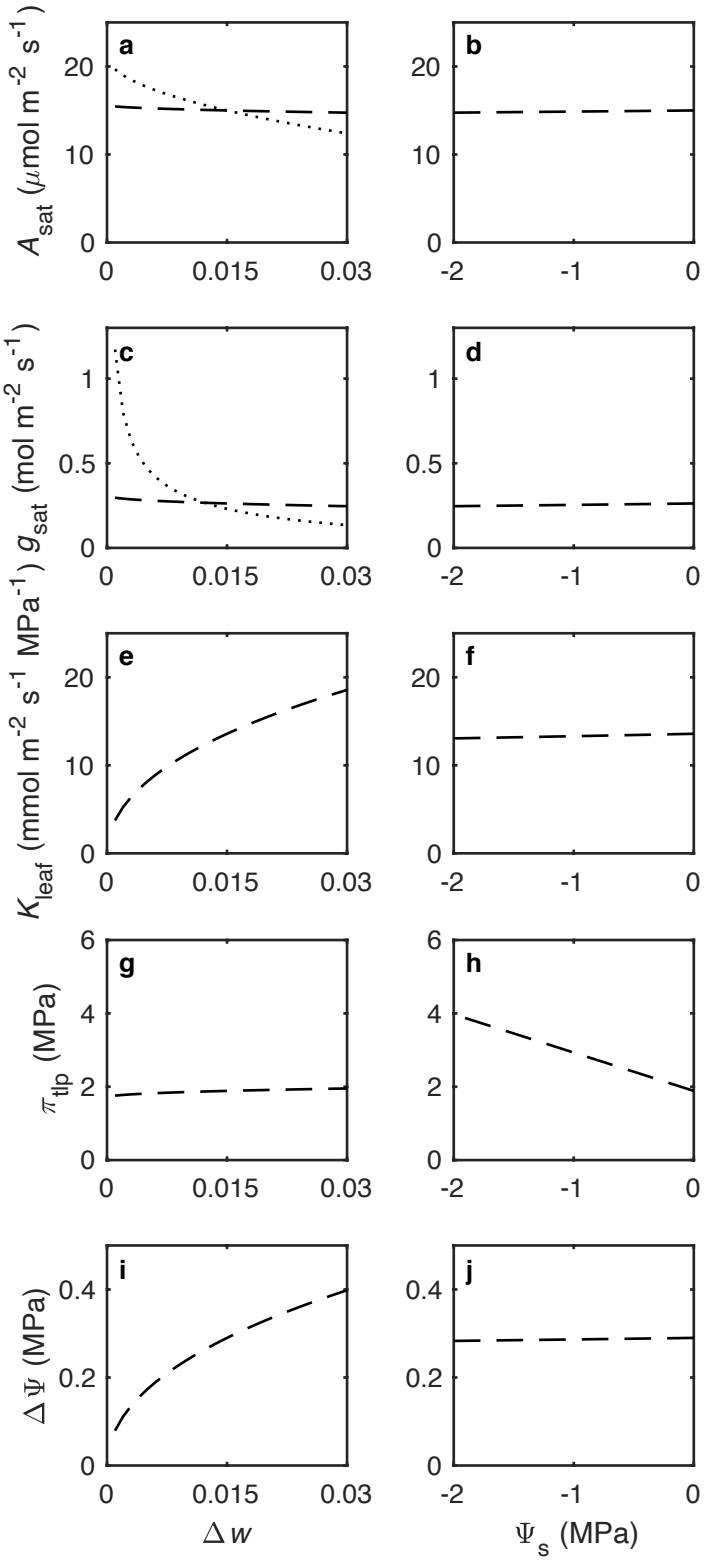
a
b
c
d
e
f
g
h
i
j
A_{sat} (μmol m^{-2} s^{-1})
g_{sat} (mol m^{-2} s^{-1})
K_{leaf} (mmol m^{-2} s^{-1} MPa^{-1})
π_{tlp} (MPa)
$\Delta\Psi$ (MPa)
Δw
Ψ_s (MPa)
0
10
20
0.5
1
2
4
6
0.2
0.4
0.015
0.03
-2
-1

1045

1046

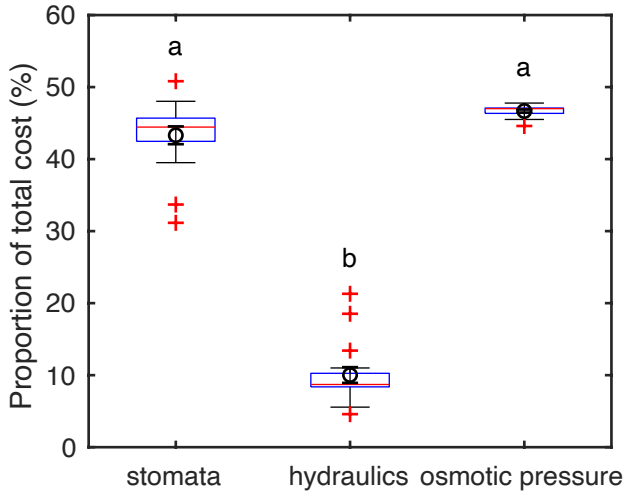
Proportion of total cost (%)
60
50
40
30
20
10
0
a
b
a
stomata
hydraulics
osmotic pressure

1047

Supplementary Methods

Derivation of the leaf optimisation model

Here we present a full derivation of the leaf optimisation model. The aim was to use optimisation of carbon gain at the leaf level to obtain average relations between A_{sat} (light-saturated CO_2 assimilation rate), g_{sat} (light saturated stomatal conductance to water vapour), K_{leaf} (leaf hydraulic conductance), π_{tlp} (leaf osmotic pressure at turgor loss point) and $\Delta\Psi$ (stem to leaf water potential difference), for changing either photosynthetic capacity (taken as V_{cmax}, the maximum carboxylation rate) or environmental conditions (Ψ_s, source water potential, to take into account the combined effects soil drying and other plant hydraulic resistances; or Δw, vapour mole fraction difference, i.e. vapour pressure difference normalised for atmospheric pressure, as a proxy for atmospheric drying).

It was assumed plants aim to maximise carbon gain per leaf area (C_{gain}). Carbon income for the leaf was taken as the mean CO_2 assimilation rate over a time period. This was represented as $A_{sat}f$, where f represents the effective fraction of time that photosynthesis is operating at A_{sat}. Costs encompassed the carbon costs of building and maintaining physiological traits for photosynthesis, so that net carbon gain was

$$C_{\mathrm{gain}} = A_{\mathrm{sat}} f - costs, \quad (1)$$

such that

$$f = \frac{\int_{t_1}^{t_2} A(t)\mathrm{d}t}{\int_{t_1}^{t_2} A_{\mathrm{sat}}\mathrm{d}t}, \quad (2)$$

where $A(t)$ is the CO_2 assimilation rate per leaf area at time t and t_1 and t_2 represent some large time interval of active leaf function.

The gain of carbon in this optimisation is expressed as a net rate of CO_2 uptake per unit leaf area. Thus costs of traits also have to be expressed in terms of a rate of carbon cost per unit leaf area. It is important to consider what the costs of these physiological traits broadly represent.

We can consider the cost of a physiological trait to be broadly split into three components: building, continual maintenance and light-dependent maintenance costs. Building costs are those required to construct the trait in question. Considered as a rate of carbon cost per leaf area, building costs represent the carbon cost to construct the trait per leaf area, spread out over the lifespan of the leaf. Continual maintenance costs represent the metabolic energetic cost required to maintain a trait whether the plant is photosynthesising or not, such as the continual maintenance of osmotic gradients across cell membranes. Light-dependent maintenance costs represent maintenance costs that are higher when the plant is photosynthesising, such as maintaining higher osmotic pressures in guard cells of stomata in the light. It is expected that these costs should be proportional to some function of the particular trait in question.

If we consider carbon gain over an arbitrary time period T, the balance of carbon income and costs can be represented as

$$C_{\text{gain}}T = A_{\text{sat}}fT - \sum_{\text{traits}}\left(\mu_{\text{b}}\frac{T}{\tau} + \mu_{\text{mc}}T + \mu_{\text{ml}}fT\right)h_{\text{trait}}, \qquad \text{(S1)}$$

where μ_{b}, μ_{mc} and μ_{ml} represent the proportionality constants for building, continual maintenance and light-dependence maintenance costs, respectively, h_{trait} is the functional dependence of costs on the trait, and τ is mean leaf lifespan. Dividing through equation S1 by the time period T gives

$$C_{\text{gain}} = A_{\text{sat}}f - \sum_{\text{traits}}\left(\frac{\mu_{\text{b}}}{\tau} + \mu_{\text{mc}} + \mu_{\text{ml}}f\right)h_{\text{trait}}. \qquad \text{(3)}$$

Thus we can see the carbon costs for each trait are made up of a building cost per leaf lifespan, a continual maintenance cost and a maintenance cost modulated by the effective fraction of time photosynthesis is operating at A_{sat}. Note that some of these component costs might be small or zero for different traits.

In practice, not all of μ_b, μ_{mc} or μ_{ml} are known for each trait, nor are f or τ necessarily known for a leaf either. It is then perhaps best to group unknowns into common parameters and do the optimisation not in terms of C_{gain} but in terms of $F = C_{gain}/f$,

$$F = \frac{C_{\text{gain}}}{f} = A_{\text{sat}} - \sum_{\text{traits}} \frac{1}{f}\left(\frac{\mu_{\text{b}}}{\tau} + \mu_{\text{mc}} + \mu_{\text{ml}} f\right) h_{\text{trait}}, \quad \text{(S2)}$$

or

$$F = A_{\text{sat}} - \sum_{\text{traits}} \mu_{\text{trait}} h_{\text{trait}}. \quad \text{(4)}$$

An expression for A_{sat} is required, and identification of the key physiological traits. Taking the Rubisco limited expression for A, and ignoring R_d (day respiration) for both simplicity and that it should be a part of maintenance costs, we have

$$A_{\text{sat}} = \frac{V_{\text{cmax}}(C_{\text{i}} - \Gamma^*)}{C_{\text{i}} + K_{\text{m}}}, \quad \text{(S3)}$$

where C_i is the internal concentration of CO_2, Γ^* is the CO_2 compensation point in the absence of R_d and K_m is the Michaelis-Menten constant for CO_2, taking into account the concentration of O_2. Here it is also assumed that mesophyll conductance to CO_2 is infinite for simplicity.

Equation S3 was linearised for algebraic simplicity, in aid of obtaining more-analytic solutions. Linearising equation S3 around $C_i = \Gamma^*$ gives

$$A_{\text{sat}} \approx \left.\frac{V_{\text{cmax}}(C_{\text{i}} - \Gamma^*)}{C_{\text{i}} + K_{\text{m}}}\right|_{C_{\text{i}} = \Gamma^*} + \left.\frac{dA_{\text{sat}}}{dC_{\text{i}}}\right|_{C_{\text{i}} = \Gamma^*} (C_{\text{i}} - \Gamma^*).$$

Now,

$$\frac{dA_{\text{sat}}}{dC_{\text{i}}} = \frac{V_{\text{cmax}}}{C_{\text{i}} + K_{\text{m}}} - \frac{V_{\text{cmax}}(C_{\text{i}} - \Gamma^*)}{(C_{\text{i}} + K_{\text{m}})^2}$$

$$\frac{dA_{\mathrm{sat}}}{dC_{\mathrm{i}}} = \frac{V_{\mathrm{cmax}}(C_{\mathrm{i}}+K_{\mathrm{m}}-C_{\mathrm{i}}+\Gamma^*)}{(C_{\mathrm{i}}+K_{\mathrm{m}})^2}$$

$$\frac{dA_{\mathrm{sat}}}{dC_{\mathrm{i}}} = \frac{V_{\mathrm{cmax}}(K_{\mathrm{m}}+\Gamma^*)}{(C_{\mathrm{i}}+K_{\mathrm{m}})^2},$$

so that

$$\left.\frac{dA_{\mathrm{sat}}}{dC_{\mathrm{i}}}\right|_{C_{\mathrm{i}}=\Gamma^*} = \frac{V_{\mathrm{cmax}}(K_{\mathrm{m}}+\Gamma^*)}{(\Gamma^*+K_{\mathrm{m}})^2}$$

$$\left.\frac{dA_{\mathrm{sat}}}{dC_{\mathrm{i}}}\right|_{C_{\mathrm{i}}=\Gamma^*} = \frac{V_{\mathrm{cmax}}}{(K_{\mathrm{m}}+\Gamma^*)},$$

giving

$$A_{\mathrm{sat}} \approx \frac{V_{\mathrm{cmax}}(\Gamma^*-\Gamma^*)}{\Gamma^*+K_{\mathrm{m}}} + \frac{V_{\mathrm{cmax}}}{K_{\mathrm{m}}+\Gamma^*}(C_{\mathrm{i}} - \Gamma^*),$$

or

$$A_{\mathrm{sat}} \approx \frac{V_{\mathrm{cmax}}}{K_{\mathrm{m}}+\Gamma^*}(C_{\mathrm{i}} - \Gamma^*). \quad \text{(S4)}$$

Equation S4 can be expressed as

$$A_{\mathrm{sat}} = k(C_{\mathrm{i}} - \Gamma^*), \quad (5)$$

where

$$k = \frac{V_{\mathrm{cmax}}}{K_{\mathrm{m}}+\Gamma^*}. \quad (6)$$

We next require a way to eliminate C_{i}. By Fick's Law and assuming infinite boundary layer conductance for simplicity, we have

$$A_{\mathrm{sat}} = \frac{g_{\mathrm{sat}}}{1.6}(C_{\mathrm{a}} - C_{\mathrm{i}}), \quad (7)$$

where the 1.6 factor is to convert g_{sat} from stomatal conductance to water vapour to the stomatal conductance to CO_2 and C_{a} is the CO_2 concentration in the surrounding air. Rearranging gives

$$C_{\mathrm{i}} = C_{\mathrm{a}} - \frac{1.6A_{\mathrm{sat}}}{g_{\mathrm{sat}}}. \quad \text{(S5)}$$

Substituting equation S5 into equation 5 gives

$$A_{\mathrm{sat}} = k\left(C_{\mathrm{a}} - \frac{1.6A}{g_{\mathrm{sat}}} - \Gamma^*\right)$$

$$A_{\mathrm{sat}}\left(1+\frac{1.6k}{g_{\mathrm{sat}}}\right)=k(C_{\mathrm{a}}-\Gamma^{*})$$

$$A_{\mathrm{sat}}=\frac{k(C_{\mathrm{a}}-\Gamma^{*})}{1+\frac{1.6k}{g_{\mathrm{sat}}}},$$

or

$$A_{\mathrm{sat}}=\frac{kg_{\mathrm{sat}}(C_{\mathrm{a}}-\Gamma^{*})}{1.6k+g_{\mathrm{sat}}}. \quad (8)$$

An expression for g_{sat} is now required. It is assumed that variation in g_{sat} is achieved, or appears to be achieved, hydraulically. Moreover, it is assumed that g_{sat} is a linear function of leaf turgor pressure (P), such that stomata are fully closed when a leaf has reached turgor loss point. That is,

$$g_{\mathrm{sat}}=\chi P, \quad (9)$$

where χ is the constant of proportionality. If it is assumed stomata are approximately the same size, χ becomes indicative of stomatal density.

Leaf turgor pressure is the result of the conflicting effects of leaf osmotic pressure (π) and leaf water potential (Ψ_{l}) and can be calculated as

$$P=\pi+\Psi_{\mathrm{l}}. \quad (10)$$

However, leaf osmotic pressure is approximately dependent on the concentration of osmolytes within leaf cells and can therefore change as the volume of a cell changes with hydration or dehydration. If the total amount of osmotic pressure is constant, π can be written as

$$\pi=\frac{\pi_{\mathrm{tlp}}V_{\mathrm{tlp}}}{V}, \quad (11)$$

where the reference is taken as the turgor loss point, such that V_{tlp} is the cell volume at turgor loss point and V is the current cell volume.

V can be calculated using the elastic modulus (ε). From the definition of elastic modulus, we have

$$\varepsilon = V\frac{dP}{dV}. \quad (12)$$

The derivative in equation 12 can be approximated by a finite difference around the turgor loss point so that equation 12 becomes

$$\varepsilon = V\frac{P-P_{\mathrm{tlp}}}{V-V_{\mathrm{tlp}}} = \frac{VP}{V-V_{\mathrm{tlp}}},$$

as P_{tlp} is zero, by definition, such that

$$V = \frac{\varepsilon V_{\mathrm{tlp}}}{\varepsilon - P},$$

so that equation 11 becomes

$$\pi = \frac{\pi_{\mathrm{tlp}} V_{\mathrm{tlp}}(\varepsilon - P)}{\varepsilon V_{\mathrm{tlp}}} = \pi_{\mathrm{tlp}}\left(1 - \frac{P}{\varepsilon}\right). \quad (S6)$$

Substituting equation S6 into equation 10 gives

$$P = \pi_{\mathrm{tlp}}\left(1 - \frac{P}{\varepsilon}\right) + \Psi_{\mathrm{l}}$$

$$\left(1 + \frac{\pi_{\mathrm{tlp}}}{\varepsilon}\right)P = \pi_{\mathrm{tlp}} + \Psi_{\mathrm{l}}$$

$$P = \frac{\pi_{\mathrm{tlp}} + \Psi_{\mathrm{l}}}{\left(1 + \frac{\pi_{\mathrm{tlp}}}{\varepsilon}\right)}. \quad (13)$$

Substituting this equation into equation 9 gives

$$g_{\mathrm{sat}} = \frac{\chi(\pi_{\mathrm{tlp}} + \Psi_{\mathrm{l}})}{\left(1 + \frac{\pi_{\mathrm{tlp}}}{\varepsilon}\right)}. \quad (S7)$$

An expression for Ψ_{l} is now required. At steady state, liquid (J) and vapour (E) fluxes of water into and out of the leaf are equal; that is

$$J = K_{\mathrm{leaf}}\Delta\Psi = K_{\mathrm{leaf}}(\Psi_{\mathrm{s}} - \Psi_{\mathrm{l}}) = E = g_{\mathrm{sat}}\Delta w, \quad (14)$$

so that

$$\Psi_{\mathrm{l}} = \Psi_{\mathrm{s}} - \frac{g_{\mathrm{sat}}\Delta w}{K_{\mathrm{leaf}}}. \quad (15)$$

Substituting equation 15 into equation S7 gives

$$g_{\mathrm{sat}} = \frac{\chi\left(\pi_{\mathrm{tlp}} + \Psi_{\mathrm{s}} - \frac{g_{\mathrm{sat}}\Delta w}{K_{\mathrm{leaf}}}\right)}{\left(1 + \frac{\pi_{\mathrm{tlp}}}{\varepsilon}\right)}$$

$$g_{\mathrm{sat}}\left[1+\frac{\frac{\chi\Delta w}{K_{\mathrm{leaf}}}}{\left(1+\frac{\pi_{\mathrm{tlp}}}{\varepsilon}\right)}\right]=\frac{\chi(\pi_{\mathrm{tlp}}+\Psi_{\mathrm{s}})}{\left(1+\frac{\pi_{\mathrm{tlp}}}{\varepsilon}\right)}$$

$$g_{\mathrm{sat}}=\frac{\chi(\pi_{\mathrm{tlp}}+\Psi_{\mathrm{s}})}{\left(1+\frac{\pi_{\mathrm{tlp}}}{\varepsilon}\right)\left[1+\frac{\frac{\chi\Delta w}{K_{\mathrm{leaf}}}}{\left(1+\frac{\pi_{\mathrm{tlp}}}{\varepsilon}\right)}\right]}$$

$$g_{\mathrm{sat}}=\frac{\chi(\pi_{\mathrm{tlp}}+\Psi_{\mathrm{s}})}{\left(1+\frac{\pi_{\mathrm{tlp}}}{\varepsilon}\right)+\frac{\chi\Delta w}{K_{\mathrm{leaf}}}},$$

or

$$g_{\mathrm{sat}}=\frac{\chi K_{\mathrm{leaf}}(\pi_{\mathrm{tlp}}+\Psi_{\mathrm{s}})}{K_{\mathrm{leaf}}\left(1+\frac{\pi_{\mathrm{tlp}}}{\varepsilon}\right)+\chi\Delta w}. \quad (16)$$

This is an equation for g_{sat} in terms of the component traits χ, K_{leaf} and π_{tlp}, ε and environmental factors Δw and Ψ_{s}.

Substituting equation 16 into equation 8 gives

$$A_{\mathrm{sat}}=\frac{k(C_{\mathrm{a}}-\Gamma^{*})\chi K_{\mathrm{leaf}}(\pi_{\mathrm{tlp}}+\Psi_{\mathrm{s}})}{\left[K_{\mathrm{leaf}}\left(1+\frac{\pi_{\mathrm{tlp}}}{\varepsilon}\right)+\chi\Delta w\right]\left[1.6k+\frac{\chi K_{\mathrm{leaf}}(\pi_{\mathrm{tlp}}+\Psi_{\mathrm{s}})}{K_{\mathrm{leaf}}\left(1+\frac{\pi_{\mathrm{tlp}}}{\varepsilon}\right)+\chi\Delta w}\right]},$$

or

$$A_{\mathrm{sat}}=\frac{k(C_{\mathrm{a}}-\Gamma^{*})\chi K_{\mathrm{leaf}}(\pi_{\mathrm{tlp}}+\Psi_{\mathrm{s}})}{1.6k\left[K_{\mathrm{leaf}}\left(1+\frac{\pi_{\mathrm{tlp}}}{\varepsilon}\right)+\chi\Delta w\right]+\chi K_{\mathrm{leaf}}(\pi_{\mathrm{tlp}}+\Psi_{\mathrm{s}})}. \quad (17)$$

The equation for A_{sat} can now be used in the equation for F.

Expressions for the costs of stomata (χ), leaf hydraulics (K_{leaf}) and osmotic pressure at turgor loss point (π_{tlp}) are still required. We will now consider how the cost of each trait should scale for stomata, leaf hydraulics and osmotic pressure.

If stomata are approximately the same size, χ is indicative of stomatal density, an area property. The carbon cost of building and maintaining stomata on the leaf surface per area should therefore be proportional to stomatal density and χ, such that

$$cost_{\chi}=\mu_{\chi}\chi, \quad (18)$$

where μ_{χ} is the constant of proportionality, or the cost parameter for χ.

How the carbon cost of hydraulics should scale with K_{leaf} is less clear, partly from differences in xylem anatomy, leaf depth and venation pattern. For simplicity and to account for both single and multiple vein anatomies, it was assumed the carbon cost of K_{leaf} scaled linearly with K_{leaf}, as K_{leaf} is also a per area quantity. That is

$$cost_{\mathrm{K}} = \mu_{\mathrm{K}} K_{\mathrm{leaf}}, \tag{19}$$

where μ_{K} is the cost parameter for K_{leaf}.

The cost of osmotic pressure should be approximately proportional to the amount of solute in the leaf per unit leaf area. However, what is driving the physiology is π_{tlp}, not total solutes per se. Therefore of two leaves with the same π_{tlp}, the one with a thicker layer of cells will have a larger cost of osmotic pressure. If it is assumed plants increase photosynthetic capacity by increasing the depth of cells, as is typical for sun-shade transitions, the cost of osmotic pressure is

$$cost_{\pi} = \mu_{\pi} \pi_{\mathrm{tlp}} \frac{k}{v}, \tag{20}$$

where μ_{π} is the cost parameter for π_{tlp} and v is the k per depth of photosynthetic tissue. Note that k/v has units of depth.

From equations 17-20, equation 4 becomes

$$F = \frac{k(C_{\mathrm{a}} - \Gamma^{*})\chi K_{\mathrm{leaf}}(\pi_{\mathrm{tlp}} + \Psi_{\mathrm{s}})}{1.6k\left[K_{\mathrm{leaf}}\left(1 + \frac{\pi_{\mathrm{tlp}}}{\varepsilon}\right) + \chi \Delta w\right] + \chi K_{\mathrm{leaf}}(\pi_{\mathrm{tlp}} + \Psi_{\mathrm{s}})} - \mu_{\chi}\chi - \mu_{\mathrm{K}} K_{\mathrm{leaf}} - \frac{\mu_{\pi}}{v}\pi_{\mathrm{tlp}} k. \tag{21}$$

F is a maximum when

$$\nabla F = \underline{0}, \tag{22a}$$

or

$$\frac{\partial F}{\partial \chi} = \frac{\partial F}{\partial K_{\mathrm{leaf}}} = \frac{\partial F}{\partial \pi_{\mathrm{tlp}}} = 0. \tag{22b}$$

Differentiating with respect to χ gives

$$\frac{k(C_a-\Gamma^*)K_{leaf}(\pi_{tlp}+\Psi_s)}{1.6k\left[K_{leaf}\left(1+\frac{\pi_{tlp}}{\varepsilon}\right)+\chi\Delta w\right]+\chi K_{leaf}(\pi_{tlp}+\Psi_s)} - \frac{k(C_a-\Gamma^*)\chi K_{leaf}(\pi_{tlp}+\Psi_s)[1.6k\Delta w+K_{leaf}(\pi_{tlp}+\Psi_s)]}{\left\{1.6k\left[K_{leaf}\left(1+\frac{\pi_{tlp}}{\varepsilon}\right)+\chi\Delta w\right]+\chi K_{leaf}(\pi_{tlp}+\Psi_s)\right\}^2} -$$

$$\mu_\chi = 0$$

$$\mu_\chi = \frac{k(C_a-\Gamma^*)K_{leaf}(\pi_{tlp}+\Psi_s)}{\left\{1.6k\left[K_{leaf}\left(1+\frac{\pi_{tlp}}{\varepsilon}\right)+\chi\Delta w\right]+\chi K_{leaf}(\pi_{tlp}+\Psi_s)\right\}^2}\left\{1.6k\left[K_{leaf}\left(1+\frac{\pi_{tlp}}{\varepsilon}\right)+\chi\Delta w\right]+\right.$$

$$\left.\chi K_{leaf}(\pi_{tlp}+\Psi_s) - 1.6k\chi\Delta w - \chi K_{leaf}(\pi_{tlp}+\Psi_s)\right\}$$

$$\mu_\chi = \frac{1.6k^2(C_a-\Gamma^*)K_{leaf}^2(\pi_{tlp}+\Psi_s)\left(1+\frac{\pi_{tlp}}{\varepsilon}\right)}{\left\{1.6k\left[K_{leaf}\left(1+\frac{\pi_{tlp}}{\varepsilon}\right)+\chi\Delta w\right]+\chi K_{leaf}(\pi_{tlp}+\Psi_s)\right\}^2}. \quad \text{(S8)}$$

Differentiating with respect to K_{leaf} gives

$$\frac{k(C_a-\Gamma^*)\chi(\pi_{tlp}+\Psi_s)}{1.6k\left[K_{leaf}\left(1+\frac{\pi_{tlp}}{\varepsilon}\right)+\chi\Delta w\right]+\chi K_{leaf}(\pi_{tlp}+\Psi_s)} -$$

$$\frac{k(C_a-\Gamma^*)\chi K_{leaf}(\pi_{tlp}+\Psi_s)\left[1.6k\left(1+\frac{\pi_{tlp}}{\varepsilon}\right)+\chi(\pi_{tlp}+\Psi_s)\right]}{\left\{1.6k\left[K_{leaf}\left(1+\frac{\pi_{tlp}}{\varepsilon}\right)+\chi\Delta w\right]+\chi K_{leaf}(\pi_{tlp}+\Psi_s)\right\}^2} - \mu_K = 0$$

$$\mu_K = \frac{k(C_a-\Gamma^*)\chi(\pi_{tlp}+\Psi_s)}{\left\{1.6k\left[K_{leaf}\left(1+\frac{\pi_{tlp}}{\varepsilon}\right)+\chi\Delta w\right]+\chi K_{leaf}(\pi_{tlp}+\Psi_s)\right\}^2}\left\{1.6k\left[K_{leaf}\left(1+\frac{\pi_{tlp}}{\varepsilon}\right)+\chi\Delta w\right]+\right.$$

$$\left.\chi K_{leaf}(\pi_{tlp}+\Psi_s) - 1.6kK_{leaf}\left(1+\frac{\pi_{tlp}}{\varepsilon}\right) - \chi K_{leaf}(\pi_{tlp}+\Psi_s)\right\}$$

$$\mu_K = \frac{1.6k^2(C_a-\Gamma^*)\chi^2\Delta w(\pi_{tlp}+\Psi_s)}{\left\{1.6k\left[K_{leaf}\left(1+\frac{\pi_{tlp}}{\varepsilon}\right)+\chi\Delta w\right]+\chi K_{leaf}(\pi_{tlp}+\Psi_s)\right\}^2}. \quad \text{(S9)}$$

Differentiating with respect to π_{tlp} gives

$$\frac{k(C_a-\Gamma^*)\chi K_{leaf}}{1.6k\left[K_{leaf}\left(1+\frac{\pi_{tlp}}{\varepsilon}\right)+\chi\Delta w\right]+\chi K_{leaf}(\pi_{tlp}+\Psi_s)} - \frac{k(C_a-\Gamma^*)\chi K_{leaf}(\pi_{tlp}+\Psi_s)\left(\frac{1.6kK_{leaf}}{\varepsilon}+\chi K_{leaf}\right)}{\left\{1.6k\left[K_{leaf}\left(1+\frac{\pi_{tlp}}{\varepsilon}\right)+\chi\Delta w\right]+\chi K_{leaf}(\pi_{tlp}+\Psi_s)\right\}^2} -$$

$$\frac{\mu_\pi}{v}k = 0$$

$$\frac{\mu_\pi}{v}k = \frac{k(C_a-\Gamma^*)\chi K_{leaf}}{\left\{1.6k\left[K_{leaf}\left(1+\frac{\pi_{tlp}}{\varepsilon}\right)+\chi\Delta w\right]+\chi K_{leaf}(\pi_{tlp}+\Psi_s)\right\}^2}\left\{1.6k\left[K_{leaf}\left(1+\frac{\pi_{tlp}}{\varepsilon}\right)+\chi\Delta w\right]+\right.$$

$$\left.\chi K_{leaf}(\pi_{tlp}+\Psi_s) - \frac{1.6kK_{leaf}(\pi_{tlp}+\Psi_s)}{\varepsilon} - \chi K_{leaf}(\pi_{tlp}+\Psi_s)\right\}$$

$$\frac{\mu_\pi}{v}k = \frac{1.6k^2(C_a-\Gamma^*)\chi K_{leaf}\left[K_{leaf}\left(1-\frac{\Psi_s}{\varepsilon}\right)+\chi\Delta w\right]}{\left\{1.6k\left[K_{leaf}\left(1+\frac{\pi_{tlp}}{\varepsilon}\right)+\chi\Delta w\right]+\chi K_{leaf}(\pi_{tlp}+\Psi_s)\right\}^2}. \quad \text{(S10)}$$

To look at possible coordination of traits it is useful to express the above equations in terms of A_{sat} and eliminate k. Noting that

$$A_{\mathrm{sat}}^2 = \frac{k^2(C_\mathrm{a}-\Gamma^*)^2\chi^2K_{\mathrm{leaf}}^2\left(\pi_{\mathrm{tlp}}+\Psi_\mathrm{s}\right)^2}{\left\{1.6k\left[K_{\mathrm{leaf}}\left(1+\frac{\pi_{\mathrm{tlp}}}{\varepsilon}\right)+\chi\Delta w\right]+\chi K_{\mathrm{leaf}}\left(\pi_{\mathrm{tlp}}+\Psi_\mathrm{s}\right)\right\}^2}, \tag{S11}$$

the above equations for cost parameters can be expressed as

$$\mu_\chi = \frac{1.6\left(1+\frac{\pi_{\mathrm{tlp}}}{\varepsilon}\right)}{(C_\mathrm{a}-\Gamma^*)\left(\pi_{\mathrm{tlp}}+\Psi_\mathrm{s}\right)\chi^2}A_{\mathrm{sat}}^2, \tag{23}$$

$$\mu_\mathrm{K} = \frac{1.6\Delta w}{(C_\mathrm{a}-\Gamma^*)\left(\pi_{\mathrm{tlp}}+\Psi_\mathrm{s}\right)K_{\mathrm{leaf}}^2}A_{\mathrm{sat}}^2, \tag{24}$$

and

$$\frac{\mu_\pi}{v} = \frac{1.6\left[K_{\mathrm{leaf}}\left(1-\frac{\Psi_\mathrm{s}}{\varepsilon}\right)+\chi\Delta w\right]}{k(C_\mathrm{a}-\Gamma^*)\left(\pi_{\mathrm{tlp}}+\Psi_\mathrm{s}\right)^2\chi K_{\mathrm{leaf}}}A_{\mathrm{sat}}^2. \tag{25a}$$

k can be eliminated in equation 25a by rearranging equation 17 as

$$1.6k\left[K_{\mathrm{leaf}}\left(1+\frac{\pi_{\mathrm{tlp}}}{\varepsilon}\right)+\chi\Delta w\right]A_{\mathrm{sat}}+\chi K_{\mathrm{leaf}}\left(\pi_{\mathrm{tlp}}+\Psi_\mathrm{s}\right)A_{\mathrm{sat}} = k(C_\mathrm{a}-\Gamma^*)\chi K_{\mathrm{leaf}}\left(\pi_{\mathrm{tlp}}+\Psi_\mathrm{s}\right)$$

$$k\left\{(C_\mathrm{a}-\Gamma^*)\chi K_{\mathrm{leaf}}\left(\pi_{\mathrm{tlp}}+\Psi_\mathrm{s}\right)-1.6A_{\mathrm{sat}}\left[K_{\mathrm{leaf}}\left(1+\frac{\pi_{\mathrm{tlp}}}{\varepsilon}\right)+\chi\Delta w\right]\right\} = \chi K_{\mathrm{leaf}}\left(\pi_{\mathrm{tlp}}+\Psi_\mathrm{s}\right)A_{\mathrm{sat}}$$

$$k = \frac{\chi K_{\mathrm{leaf}}\left(\pi_{\mathrm{tlp}}+\Psi_\mathrm{s}\right)A_{\mathrm{sat}}}{(C_\mathrm{a}-\Gamma^*)\chi K_{\mathrm{leaf}}\left(\pi_{\mathrm{tlp}}+\Psi_\mathrm{s}\right)-1.6A_{\mathrm{sat}}\left[K_{\mathrm{leaf}}\left(1+\frac{\pi_{\mathrm{tlp}}}{\varepsilon}\right)+\chi\Delta w\right]}, \tag{35}$$

so that

$$\frac{\mu_\pi}{v} = \frac{1.6\left[K_{\mathrm{leaf}}\left(1-\frac{\Psi_\mathrm{s}}{\varepsilon}\right)+\chi\Delta w\right]\left\{(C_\mathrm{a}-\Gamma^*)\chi K_{\mathrm{leaf}}\left(\pi_{\mathrm{tlp}}+\Psi_\mathrm{s}\right)-1.6A_{\mathrm{sat}}\left[K_{\mathrm{leaf}}\left(1+\frac{\pi_{\mathrm{tlp}}}{\varepsilon}\right)+\chi\Delta w\right]\right\}}{(C_\mathrm{a}-\Gamma^*)\left(\pi_{\mathrm{tlp}}+\Psi_\mathrm{s}\right)^3\chi^2K_{\mathrm{leaf}}^2}A_{\mathrm{sat}}. \tag{25b}$$

The equations for the cost parameters can now be solved for the traits, given A_{sat}. From equations 23 and 24 it follows that

$$\frac{\mu_\chi}{\mu_\mathrm{K}} = \frac{\left(1+\frac{\pi_{\mathrm{tlp}}}{\varepsilon}\right)K_{\mathrm{leaf}}^2}{\Delta w\chi^2}, \tag{S12}$$

so that

$$K_{\text{leaf}}^2 = \frac{\mu_\chi \Delta w}{\mu_K\left(1+\frac{\pi_{\text{tlp}}}{\varepsilon}\right)}\chi^2,$$

or

$$K_{\text{leaf}} = \left[\frac{\mu_\chi \Delta w}{\mu_K\left(1+\frac{\pi_{\text{tlp}}}{\varepsilon}\right)}\right]^{\frac{1}{2}}\chi. \tag{S13}$$

Substituting equation S13 into equation 25b, but first writing $K_{\text{leaf}} = \alpha\chi$, gives

$$\frac{\mu_\pi}{v} = \frac{1.6\left[\alpha\chi\left(1-\frac{\Psi_s}{\varepsilon}\right)+\chi\Delta w\right]\left\{(C_a-\Gamma^*)\chi\alpha\chi(\pi_{\text{tlp}}+\Psi_s)-1.6A_{\text{sat}}\left[\alpha\chi\left(1+\frac{\pi_{\text{tlp}}}{\varepsilon}\right)+\chi\Delta w\right]\right\}}{(C_a-\Gamma^*)(\pi_{\text{tlp}}+\Psi_s)^3\chi^2\alpha^2\chi^2}A_{\text{sat}}$$

$$\frac{\mu_\pi}{v} = \frac{1.6\left[\alpha\left(1-\frac{\Psi_s}{\varepsilon}\right)+\Delta w\right]\left\{(C_a-\Gamma^*)\alpha\chi(\pi_{\text{tlp}}+\Psi_s)-1.6A_{\text{sat}}\left[\alpha\left(1+\frac{\pi_{\text{tlp}}}{\varepsilon}\right)+\Delta w\right]\right\}}{(C_a-\Gamma^*)(\pi_{\text{tlp}}+\Psi_s)^3\alpha^2\chi^2}A_{\text{sat}}. \tag{S14}$$

From equation 23

$$\chi = \left[\frac{1.6\left(1+\frac{\pi_{\text{tlp}}}{\varepsilon}\right)}{\mu_\chi(C_a-\Gamma^*)(\pi_{\text{tlp}}+\Psi_s)}\right]^{\frac{1}{2}}A_{\text{sat}}, \tag{27}$$

which, substituting into equation S14, after writing $\chi = \beta A_{\text{sat}}$, gives

$$\frac{\mu_\pi}{v} = \frac{1.6\left[\alpha\left(1-\frac{\Psi_s}{\varepsilon}\right)+\Delta w\right]\left\{(C_a-\Gamma^*)\alpha\beta A_{\text{sat}}(\pi_{\text{tlp}}+\Psi_s)-1.6A_{\text{sat}}\left[\alpha\left(1+\frac{\pi_{\text{tlp}}}{\varepsilon}\right)+\Delta w\right]\right\}}{(C_a-\Gamma^*)(\pi_{\text{tlp}}+\Psi_s)^3\alpha^2\beta^2A_{\text{sat}}^2}A_{\text{sat}}$$

$$\frac{\mu_\pi}{v} = \frac{1.6\left[\alpha\left(1-\frac{\Psi_s}{\varepsilon}\right)+\Delta w\right]\left\{(C_a-\Gamma^*)\alpha\beta(\pi_{\text{tlp}}+\Psi_s)-1.6\left[\alpha\left(1+\frac{\pi_{\text{tlp}}}{\varepsilon}\right)+\Delta w\right]\right\}}{(C_a-\Gamma^*)(\pi_{\text{tlp}}+\Psi_s)^3\alpha^2\beta^2A_{\text{sat}}^2}A_{\text{sat}}^2$$

$$\frac{\mu_\pi}{v} = \frac{1.6\left[\alpha\left(1-\frac{\Psi_s}{\varepsilon}\right)+\Delta w\right]\left\{(C_a-\Gamma^*)\alpha\beta(\pi_{\text{tlp}}+\Psi_s)-1.6\left[\alpha\left(1+\frac{\pi_{\text{tlp}}}{\varepsilon}\right)+\Delta w\right]\right\}}{(C_a-\Gamma^*)(\pi_{\text{tlp}}+\Psi_s)^3\alpha^2\beta^2}$$

$$\frac{\mu_\pi}{v} = \frac{1.6\left[\left(1-\frac{\Psi_s}{\varepsilon}\right)+\frac{\Delta w}{\alpha}\right]\left\{(C_a-\Gamma^*)\beta(\pi_{\text{tlp}}+\Psi_s)-1.6\left[\left(1+\frac{\pi_{\text{tlp}}}{\varepsilon}\right)+\frac{\Delta w}{\alpha}\right]\right\}}{(C_a-\Gamma^*)(\pi_{\text{tlp}}+\Psi_s)^3\beta^2}. \tag{S15}$$

It can already be seen here that equation S15 is an equation for π_{tlp} and that it is independent of A_{sat}.

Now,

$$\frac{\Delta w}{\alpha} = \left[\frac{\mu_K \Delta w}{\mu_\chi}\left(1+\frac{\pi_{\text{tlp}}}{\varepsilon}\right)\right]^{\frac{1}{2}}, \tag{S16}$$

so that, expanding β gives

$$\frac{\left(\frac{\mu_\pi}{v}\right)(C_a-\Gamma^*)(\pi_{tlp}+\Psi_s)^3 1.6\left(1+\frac{\pi_{tlp}}{\varepsilon}\right)}{\mu_\chi(C_a-\Gamma^*)(\pi_{tlp}+\Psi_s)} = 1.6\left\{\left(1-\frac{\Psi_s}{\varepsilon}\right)+\left[\frac{\mu_K\Delta w}{\mu_\chi}\left(1+\right.\right.\right.$$

$$\left.\left.\left.\frac{\pi_{tlp}}{\varepsilon}\right)\right]^{\frac{1}{2}}\right\}\left\{\left[\frac{1.6\left(1+\frac{\pi_{tlp}}{\varepsilon}\right)}{\mu_\chi(C_a-\Gamma^*)(\pi_{tlp}+\Psi_s)}\right]^{\frac{1}{2}}(C_a-\Gamma^*)(\pi_{tlp}+\Psi_s)-1.6\left[\left(1+\frac{\pi_{tlp}}{\varepsilon}\right)+\right.\right.$$

$$\left.\left.\left[\frac{\mu_K\Delta w}{\mu_\chi}\left(1+\frac{\pi_{tlp}}{\varepsilon}\right)\right]^{\frac{1}{2}}\right]\right\}$$

$$\frac{\left(\frac{\mu_\pi}{v}\right)}{\mu_\chi}\left(1+\frac{\pi_{tlp}}{\varepsilon}\right)(\pi_{tlp}+\Psi_s)^2-\left\{\left(1-\frac{\Psi_s}{\varepsilon}\right)+\left[\frac{\mu_K\Delta w}{\mu_\chi}\left(1+\right.\right.\right.$$

$$\left.\left.\left.\frac{\pi_{tlp}}{\varepsilon}\right)\right]^{\frac{1}{2}}\right\}\left\{\left[\frac{1.6\left(1+\frac{\pi_{tlp}}{\varepsilon}\right)(C_a-\Gamma^*)(\pi_{tlp}+\Psi_s)}{\mu_\chi}\right]^{\frac{1}{2}}-1.6\left[\left(1+\frac{\pi_{tlp}}{\varepsilon}\right)+\left[\frac{\mu_K\Delta w}{\mu_\chi}\left(1+\frac{\pi_{tlp}}{\varepsilon}\right)\right]^{\frac{1}{2}}\right]\right\}=0.$$

(26)

This is an equation for π_{tlp} in terms of cost parameters, ε and environmental conditions only; that is, π_{tlp} is independent of A_{sat}. Equation 26 needs to be solved numerically, but the solution can then be used to solve for χ and K_{leaf} for a given A_{sat}. Substituting equation 27 into equation S13 gives

$$K_{leaf}=\left[\frac{\mu_\chi\Delta w}{\mu_K\left(1+\frac{\pi_{tlp}}{\varepsilon}\right)}\right]^{\frac{1}{2}}\chi=\left[\frac{1.6\left(1+\frac{\pi_{tlp}}{\varepsilon}\right)\mu_\chi\Delta w}{\mu_K\left(1+\frac{\pi_{tlp}}{\varepsilon}\right)\mu_\chi(C_a-\Gamma^*)(\pi_{tlp}+\Psi_s)}\right]^{\frac{1}{2}}A_{sat}$$

$$K_{leaf}=\left[\frac{1.6\Delta w}{\mu_K(C_a-\Gamma^*)(\pi_{tlp}+\Psi_s)}\right]^{\frac{1}{2}}A_{sat}. \quad (28)$$

That is, K_{leaf} is proportional to A_{sat}, everything else being equal.

For typical measurements it is easier to express the solution in terms of g_{sat} instead of χ. From equations 16, 27 and 28, g_{sat} can be solved as

$$g_{\mathrm{sat}} = \left[\frac{1.6\left(1+\frac{\pi_{\mathrm{tlp}}}{\varepsilon}\right)}{\mu_\chi (C_{\mathrm{a}}-\Gamma^*)(\pi_{\mathrm{tlp}}+\Psi_{\mathrm{s}})}\right]^{\frac{1}{2}} \frac{(\pi_{\mathrm{tlp}}+\Psi_{\mathrm{s}})}{\left(1+\frac{\pi_{\mathrm{tlp}}}{\varepsilon}\right)+\left[\frac{\mu_{\mathrm{K}}\left(1+\frac{\pi_{\mathrm{tlp}}}{\varepsilon}\right)}{\mu_\chi \Delta w}\right]^{\frac{1}{2}}\Delta w} A_{\mathrm{sat}}$$

$$g_{\mathrm{sat}} = \frac{\left[\frac{1.6\left(\pi_{\mathrm{tlp}}+\Psi_{\mathrm{s}}\right)}{\mu_\chi (C_{\mathrm{a}}-\Gamma^*)\left(1+\frac{\pi_{\mathrm{tlp}}}{\varepsilon}\right)}\right]^{\frac{1}{2}}}{1+\left[\frac{\mu_{\mathrm{K}}\Delta w}{\mu_\chi\left(1+\frac{\pi_{\mathrm{tlp}}}{\varepsilon}\right)}\right]^{\frac{1}{2}}} A_{\mathrm{sat}}. \quad (29)$$

That is, g_{sat} is proportional to A_{sat} under identical conditions.

Leaf water potential can be solved for by substituting equations 28 and 29 into equation 15, as

$$\Psi_{\mathrm{l}} = \Psi_{\mathrm{s}} - \frac{\left[\frac{1.6\left(\pi_{\mathrm{tlp}}+\Psi_{\mathrm{s}}\right)\mu_{\mathrm{K}}(C_{\mathrm{a}}-\Gamma^*)\left(\pi_{\mathrm{tlp}}+\Psi_{\mathrm{s}}\right)}{\mu_\chi (C_{\mathrm{a}}-\Gamma^*)\left(1+\frac{\pi_{\mathrm{tlp}}}{\varepsilon}\right)1.6\Delta w}\right]^{\frac{1}{2}}\Delta w}{1+\left[\frac{\mu_{\mathrm{K}}\Delta w}{\mu_\chi\left(1+\frac{\pi_{\mathrm{tlp}}}{\varepsilon}\right)}\right]^{\frac{1}{2}}}$$

$$\Psi_{\mathrm{l}} = \Psi_{\mathrm{s}} - \frac{\left[\frac{\mu_{\mathrm{K}}\Delta w}{\mu_\chi\left(1+\frac{\pi_{\mathrm{tlp}}}{\varepsilon}\right)}\right]^{\frac{1}{2}}(\pi_{\mathrm{tlp}}+\Psi_{\mathrm{s}})}{1+\left[\frac{\mu_{\mathrm{K}}\Delta w}{\mu_\chi\left(1+\frac{\pi_{\mathrm{tlp}}}{\varepsilon}\right)}\right]^{\frac{1}{2}}},$$

or

$$\Delta\Psi = \Psi_{\mathrm{s}} - \Psi_{\mathrm{l}} = \frac{(\pi_{\mathrm{tlp}}+\Psi_{\mathrm{s}})}{\left[\frac{\mu_\chi\left(1+\frac{\pi_{\mathrm{tlp}}}{\varepsilon}\right)}{\mu_{\mathrm{K}}\Delta w}\right]^{\frac{1}{2}}+1}. \quad (30)$$

It is more useful to express the optimal solution in terms of k for modelling the effect of different environmental conditions on adaptive π_{tlp}, χ and K_{leaf}, and in turn A_{sat} and g_{sat}. The equation for π_{tlp} in this case is the same as equation 26 because π_{tlp} is independent of both A_{sat} and k. Substituting equation S13 into equation S8 gives

$$\mu_\chi = \frac{1.6k^2(C_{\mathrm{a}}-\Gamma^*)\alpha^2\chi^2\left(\pi_{\mathrm{tlp}}+\Psi_{\mathrm{s}}\right)\left(1+\frac{\pi_{\mathrm{tlp}}}{\varepsilon}\right)}{\left\{1.6k\left[\alpha\chi\left(1+\frac{\pi_{\mathrm{tlp}}}{\varepsilon}\right)+\chi\Delta w\right]+\chi\alpha\chi(\pi_{\mathrm{tlp}}+\Psi_{\mathrm{s}})\right\}^2}$$

$$\mu_\chi = \frac{1.6k^2(C_a-\Gamma^*)(\pi_{tlp}+\Psi_s)\left(1+\frac{\pi_{tlp}}{\varepsilon}\right)}{\left\{1.6k\left[\left(1+\frac{\pi_{tlp}}{\varepsilon}\right)+\frac{\Delta w}{\alpha}\right]+\chi(\pi_{tlp}+\Psi_s)\right\}^2}$$

$$1.6k\left[\left(1+\frac{\pi_{tlp}}{\varepsilon}\right)+\frac{\Delta w}{\alpha}\right]+\chi(\pi_{tlp}+\Psi_s)=k\left[\frac{1.6(C_a-\Gamma^*)(\pi_{tlp}+\Psi_s)\left(1+\frac{\pi_{tlp}}{\varepsilon}\right)}{\mu_\chi}\right]^{\frac{1}{2}}$$

$$\chi = k\left\{\left[\frac{1.6(C_a-\Gamma^*)\left(1+\frac{\pi_{tlp}}{\varepsilon}\right)}{\mu_\chi(\pi_{tlp}+\Psi_s)}\right]^{\frac{1}{2}}-\frac{1.6}{(\pi_{tlp}+\Psi_s)}\left[\left(1+\frac{\pi_{tlp}}{\varepsilon}\right)+\frac{\Delta w}{\alpha}\right]\right\}$$

$$\chi = k\left\{\left[\frac{1.6(C_a-\Gamma^*)\left(1+\frac{\pi_{tlp}}{\varepsilon}\right)}{\mu_\chi(\pi_{tlp}+\Psi_s)}\right]^{\frac{1}{2}}-\frac{1.6}{(\pi_{tlp}+\Psi_s)}\left[\left(1+\frac{\pi_{tlp}}{\varepsilon}\right)+\left[\frac{\mu_K\Delta w}{\mu_\chi}\left(1+\frac{\pi_{tlp}}{\varepsilon}\right)\right]^{\frac{1}{2}}\right]\right\}$$

$$\chi = k\frac{1.6\left(1+\frac{\pi_{tlp}}{\varepsilon}\right)}{(\pi_{tlp}+\Psi_s)}\left\{\left[\frac{(C_a-\Gamma^*)(\pi_{tlp}+\Psi_s)}{1.6\mu_\chi\left(1+\frac{\pi_{tlp}}{\varepsilon}\right)}\right]^{\frac{1}{2}}-\left[1+\left[\frac{\mu_K\Delta w}{\mu_\chi\left(1+\frac{\pi_{tlp}}{\varepsilon}\right)}\right]^{\frac{1}{2}}\right]\right\}. \quad (36)$$

From equation S13, K_{leaf} can then be written as

$$K_{leaf} = k\frac{1.6\left(1+\frac{\pi_{tlp}}{\varepsilon}\right)}{(\pi_{tlp}+\Psi_s)}\left[\frac{\mu_\chi\Delta w}{\mu_K\left(1+\frac{\pi_{tlp}}{\varepsilon}\right)}\right]^{\frac{1}{2}}\left\{\left[\frac{(C_a-\Gamma^*)(\pi_{tlp}+\Psi_s)}{1.6\mu_\chi\left(1+\frac{\pi_{tlp}}{\varepsilon}\right)}\right]^{\frac{1}{2}}-\left[1+\left[\frac{\mu_K\Delta w}{\mu_\chi\left(1+\frac{\pi_{tlp}}{\varepsilon}\right)}\right]^{\frac{1}{2}}\right]\right\}$$

$$K_{leaf} = k\frac{1.6}{(\pi_{tlp}+\Psi_s)}\left[\frac{\mu_\chi\Delta w\left(1+\frac{\pi_{tlp}}{\varepsilon}\right)}{\mu_K}\right]^{\frac{1}{2}}\left\{\left[\frac{(C_a-\Gamma^*)(\pi_{tlp}+\Psi_s)}{1.6\mu_\chi\left(1+\frac{\pi_{tlp}}{\varepsilon}\right)}\right]^{\frac{1}{2}}-\left[1+\left[\frac{\mu_K\Delta w}{\mu_\chi\left(1+\frac{\pi_{tlp}}{\varepsilon}\right)}\right]^{\frac{1}{2}}\right]\right\}.$$

(37)

The proportional cost of stomata, hydraulics and osmotic pressure, relative to the total cost of these three traits can be estimated. Let the denominator in equation 17 be D, such that

$$D = 1.6k\left[K_{leaf}\left(1+\frac{\pi_{tlp}}{\varepsilon}\right)+\chi\Delta w\right]+\chi K_{leaf}(\pi_{tlp}+\Psi_s). \quad (S17)$$

The total costs of stomata, hydraulics and osmotic pressure is

$$costs = \mu_\chi\chi+\mu_K K_{leaf}+\frac{\mu_\pi}{v}\pi_{tlp}k$$

$$costs = \frac{1}{D^2}\left\{1.6k^2(C_\mathrm{a} - \Gamma^*)\chi K_\mathrm{leaf}^2\left(\pi_\mathrm{tlp} + \Psi_\mathrm{s}\right)\left(1 + \frac{\pi_\mathrm{tlp}}{\varepsilon}\right) + 1.6k^2(C_\mathrm{a} - \right.$$

$$\left.\Gamma^*)\chi^2 K_\mathrm{leaf}\Delta w\left(\pi_\mathrm{tlp} + \Psi_\mathrm{s}\right) + 1.6k^2(C_\mathrm{a} - \Gamma^*)\chi K_\mathrm{leaf}\pi_\mathrm{tlp}\left[K_\mathrm{leaf}\left(1 - \frac{\Psi_\mathrm{s}}{\varepsilon}\right) + \chi\Delta w\right]\right\}$$

$$costs = \frac{1}{D^2}1.6k^2(C_\mathrm{a} - \Gamma^*)\chi K_\mathrm{leaf}\left\{K_\mathrm{leaf}\left(\pi_\mathrm{tlp} + \Psi_\mathrm{s}\right)\left(1 + \frac{\pi_\mathrm{tlp}}{\varepsilon}\right) + \chi\Delta w\left(\pi_\mathrm{tlp} + \Psi_\mathrm{s}\right) + \right.$$

$$\left.\pi_\mathrm{tlp}\left[K_\mathrm{leaf}\left(1 - \frac{\Psi_\mathrm{s}}{\varepsilon}\right) + \chi\Delta w\right]\right\}$$

$$costs = \frac{1}{D^2}1.6k^2(C_\mathrm{a} - \Gamma^*)\chi K_\mathrm{leaf}\left\{\left(\pi_\mathrm{tlp} + \Psi_\mathrm{s}\right)\left[K_\mathrm{leaf}\left(1 + \frac{\pi_\mathrm{tlp}}{\varepsilon}\right) + \chi\Delta w\right] + \right.$$

$$\left.\pi_\mathrm{tlp}\left[K_\mathrm{leaf}\left(1 - \frac{\Psi_\mathrm{s}}{\varepsilon}\right) + \chi\Delta w\right]\right\}.$$

(S18)

Thus the relative cost of stomata (p_χ) can be defined as

$$p_\chi = \frac{cost_\chi}{costs}, \tag{S19}$$

or, from equations S8 and S17-S19,

$$p_\chi = \frac{1.6k^2(C_\mathrm{a}-\Gamma^*)\chi K_\mathrm{leaf}^2\left(\pi_\mathrm{tlp}+\Psi_\mathrm{s}\right)\left(1+\frac{\pi_\mathrm{tlp}}{\varepsilon}\right)D^2}{D^2 1.6k^2(C_\mathrm{a}-\Gamma^*)\chi K_\mathrm{leaf}\left\{\left(\pi_\mathrm{tlp}+\Psi_\mathrm{s}\right)\left[K_\mathrm{leaf}\left(1+\frac{\pi_\mathrm{tlp}}{\varepsilon}\right)+\chi\Delta w\right]+\pi_\mathrm{tlp}\left[K_\mathrm{leaf}\left(1-\frac{\Psi_\mathrm{s}}{\varepsilon}\right)+\chi\Delta w\right]\right\}}$$

$$p_\chi = \frac{K_\mathrm{leaf}\left(\pi_\mathrm{tlp}+\Psi_\mathrm{s}\right)\left(1+\frac{\pi_\mathrm{tlp}}{\varepsilon}\right)}{\left\{\left(\pi_\mathrm{tlp}+\Psi_\mathrm{s}\right)\left[K_\mathrm{leaf}\left(1+\frac{\pi_\mathrm{tlp}}{\varepsilon}\right)+\chi\Delta w\right]+\pi_\mathrm{tlp}\left[K_\mathrm{leaf}\left(1-\frac{\Psi_\mathrm{s}}{\varepsilon}\right)+\chi\Delta w\right]\right\}}$$

$$p_\chi = \frac{K_\mathrm{leaf}\left(\pi_\mathrm{tlp}+\Psi_\mathrm{s}\right)}{\left\{\pi_\mathrm{tlp}K_\mathrm{leaf}+\Psi_\mathrm{s}K_\mathrm{leaf}+\pi_\mathrm{tlp}\frac{\chi\Delta w}{\left(1+\frac{\pi_\mathrm{tlp}}{\varepsilon}\right)}+\Psi_\mathrm{s}\frac{\chi\Delta w}{\left(1+\frac{\pi_\mathrm{tlp}}{\varepsilon}\right)}+\pi_\mathrm{tlp}K_\mathrm{leaf}\frac{\left(1-\frac{\Psi_\mathrm{s}}{\varepsilon}\right)}{\left(1+\frac{\pi_\mathrm{tlp}}{\varepsilon}\right)}+\pi_\mathrm{tlp}\frac{\chi\Delta w}{\left(1+\frac{\pi_\mathrm{tlp}}{\varepsilon}\right)}\right\}}$$

$$p_\chi = \frac{K_\mathrm{leaf}\left(\pi_\mathrm{tlp}+\Psi_\mathrm{s}\right)}{\pi_\mathrm{tlp}\left\{K_\mathrm{leaf}\left[1+\frac{\left(1-\frac{\Psi_\mathrm{s}}{\varepsilon}\right)}{\left(1+\frac{\pi_\mathrm{tlp}}{\varepsilon}\right)}\right]+\frac{2\chi\Delta w}{\left(1+\frac{\pi_\mathrm{tlp}}{\varepsilon}\right)}\right\}+\Psi_\mathrm{s}\left\{K_\mathrm{leaf}+\frac{\chi\Delta w}{\left(1+\frac{\pi_\mathrm{tlp}}{\varepsilon}\right)}\right\}}. \tag{31}$$

Likewise, the relative cost of hydraulics can be defined as

$$p_\mathrm{K} = \frac{cost_\mathrm{K}}{costs}, \tag{S20}$$

or, from equations S9, S17, S18 and S20,

$$p_\mathrm{K} = \frac{1.6k^2(C_\mathrm{a}-\Gamma^*)\chi^2 K_\mathrm{leaf}\Delta w\left(\pi_\mathrm{tlp}+\Psi_\mathrm{s}\right)D^2}{D^2 1.6k^2(C_\mathrm{a}-\Gamma^*)\chi K_\mathrm{leaf}\left\{\left(\pi_\mathrm{tlp}+\Psi_\mathrm{s}\right)\left[K_\mathrm{leaf}\left(1+\frac{\pi_\mathrm{tlp}}{\varepsilon}\right)+\chi\Delta w\right]+\pi_\mathrm{tlp}\left[K_\mathrm{leaf}\left(1-\frac{\Psi_\mathrm{s}}{\varepsilon}\right)+\chi\Delta w\right]\right\}}$$

$$p_{\mathrm{K}} = \frac{\chi\Delta w(\pi_{\mathrm{tlp}}+\Psi_{\mathrm{s}})}{\left\{(\pi_{\mathrm{tlp}}+\Psi_{\mathrm{s}})\left[K_{\mathrm{leaf}}\left(1+\frac{\pi_{\mathrm{tlp}}}{\varepsilon}\right)+\chi\Delta w\right]+\pi_{\mathrm{tlp}}\left[K_{\mathrm{leaf}}\left(1-\frac{\Psi_{\mathrm{s}}}{\varepsilon}\right)+\chi\Delta w\right]\right\}}$$

$$p_{\mathrm{K}} = \frac{\frac{\chi\Delta w}{\left(1+\frac{\pi_{\mathrm{tlp}}}{\varepsilon}\right)}(\pi_{\mathrm{tlp}}+\Psi_s)}{\pi_{\mathrm{tlp}}\left\{K_{\mathrm{leaf}}\left[1+\frac{\left(1-\frac{\Psi_{\mathrm{s}}}{\varepsilon}\right)}{\left(1+\frac{\pi_{\mathrm{tlp}}}{\varepsilon}\right)}\right]+\frac{2\chi\Delta w}{\left(1+\frac{\pi_{\mathrm{tlp}}}{\varepsilon}\right)}\right\}+\Psi_{\mathrm{s}}\left\{K_{\mathrm{leaf}}+\frac{\chi\Delta w}{\left(1+\frac{\pi_{\mathrm{tlp}}}{\varepsilon}\right)}\right\}}. \quad (32)$$

Finally, the relative cost of osmotic pressure can be defined as

$$p_{\pi} = \frac{cost_{\pi}}{costs}, \quad (S21)$$

or, from equations S10, S17, S18 and S21,

$$p_{\pi} = \frac{1.6k^2(C_{\mathrm{a}}-\Gamma^*)\chi K_{\mathrm{leaf}}\pi_{\mathrm{tlp}}\left[K_{\mathrm{leaf}}\left(1-\frac{\Psi_{\mathrm{s}}}{\varepsilon}\right)+\chi\Delta w\right]D^2}{D^2 1.6k^2(C_{\mathrm{a}}-\Gamma^*)\chi K_{\mathrm{leaf}}\left\{(\pi_{\mathrm{tlp}}+\Psi_{\mathrm{s}})\left[K_{\mathrm{leaf}}\left(1+\frac{\pi_{\mathrm{tlp}}}{\varepsilon}\right)+\chi\Delta w\right]+\pi_{\mathrm{tlp}}\left[K_{\mathrm{leaf}}\left(1-\frac{\Psi_{\mathrm{s}}}{\varepsilon}\right)+\chi\Delta w\right]\right\}}$$

$$p_{\pi} = \frac{\pi_{\mathrm{tlp}}\left[K_{\mathrm{leaf}}\left(1-\frac{\Psi_{\mathrm{s}}}{\varepsilon}\right)+\chi\Delta w\right]}{\left\{(\pi_{\mathrm{tlp}}+\Psi_{\mathrm{s}})\left[K_{\mathrm{leaf}}\left(1+\frac{\pi_{\mathrm{tlp}}}{\varepsilon}\right)+\chi\Delta w\right]+\pi_{\mathrm{tlp}}\left[K_{\mathrm{leaf}}\left(1-\frac{\Psi_{\mathrm{s}}}{\varepsilon}\right)+\chi\Delta w\right]\right\}}$$

$$p_{\pi} = \frac{1}{\left(1+\frac{\Psi_{\mathrm{s}}}{\pi_{\mathrm{tlp}}}\right)\left[\frac{K_{\mathrm{leaf}}\left(1+\frac{\pi_{\mathrm{tlp}}}{\varepsilon}\right)+\chi\Delta w}{K_{\mathrm{leaf}}\left(1-\frac{\Psi_{\mathrm{s}}}{\varepsilon}\right)+\chi\Delta w}\right]+1}. \quad (33)$$

Derivation of the linearised Cowan-Farquhar optimisation model

Although the linearised Cowan-Farquhar optimisation model has been derived a number of times [1-5], it is shown here for completeness.

Taking a transpiration cost view, the aim is to maximise

$$F = A - \mu_{\mathrm{E}}E, \quad (S22)$$

where μ_E is the cost parameter for transpiration. From equation 8 and assuming infinite boundary layer conductance, equation S22 can be written as

$$F = \frac{k g_s (C_a - \Gamma^*)}{1.6k + g_s} - \mu_E \Delta w g_s. \quad \text{(S23)}$$

The maximum occurs when

$$\frac{dF}{dg_s} = 0, \quad \text{(S24)}$$

giving

$$\frac{k(C_a - \Gamma^*)}{1.6k + g_s} - \frac{k g_s (C_a - \Gamma^*)}{(1.6k + g_s)^2} - \mu_E \Delta w = 0$$

$$\frac{1.6k^2 (C_a - \Gamma^*) + k g_s (C_a - \Gamma^*) - k g_s (C_a - \Gamma^*)}{(1.6k + g_s)^2} = \mu_E \Delta w$$

$$\frac{1.6k^2 (C_a - \Gamma^*)}{(1.6k + g_s)^2} = \mu_E \Delta w,$$

or

$$\mu_E = \frac{1.6k^2 (C_a - \Gamma^*)}{\Delta w (1.6k + g_s)^2}. \quad \text{(S25)}$$

Now, noting that

$$A^2 = \frac{k^2 g_s^2 (C_a - \Gamma^*)^2}{(1.6k + g_s)^2},$$

then equation S25 can be written as

$$\mu_E = \frac{1.6}{\Delta w (C_a - \Gamma^*) g_s^2} A^2, \quad \text{(38)}$$

or

$$g_s = \left[\frac{1.6}{\mu_E \Delta w (C_a - \Gamma^*)}\right]^{\frac{1}{2}} A. \quad \text{(40)}$$

To get g_s in terms of k, rearranging equation S25 gives

$$(1.6k + g_s)^2 = \frac{1.6k^2 (C_a - \Gamma^*)}{\mu_E \Delta w},$$

or

$$g_s = 1.6k \left\{\left[\frac{(C_a - \Gamma^*)}{1.6 \mu_E \Delta w}\right]^{\frac{1}{2}} - 1\right\}. \quad \text{(41)}$$

To predict how g_s and A vary with Δw for a constant k requires an equation to solve for k at a reference A and Δw. From equation 8 we get

$$kg_s(C_a - \Gamma^*) = 1.6Ak + g_sA$$

$$k[g_s(C_a - \Gamma^*) - 1.6A] = g_sA$$

$$k = \frac{g_sA}{g_s(C_a - \Gamma^*) - 1.6A}. \quad (39)$$

Estimate for the building cost of hydraulics, spread over the lifespan of the leaf

A crude estimate for the mean building cost of hydraulics can be obtained by combining estimates of vein mass fraction of total dry matter from John, et al. [6] and the average construction cost and lifespan of leaves from Navas, et al. [7]. Comparisons with estimates for the maintenance cost of cell osmotic pressure can then be made with de Vries [8]. Although both costs are evaluated on a mass basis, while costs per area are better for comparisons with the optimal model, the mean cost of hydraulics as a proportion of that of osmotic pressure should scale similarly whether done on a per area or per mass basis.

The mean building cost of hydraulics spread over the lifespan of the leaf ($cost_{Kb}$; here g glucose g^{-1} d^{-1}) can be compared with that for maintenance of osmotic pressure ($cost_{\pi m}$; here g glucose g^{-1} d^{-1}) as

$$\frac{cost_{Kb}}{cost_{\pi m}} = \left(\frac{MFV \times CC_{leaf}}{LLS}\right) \Big/ cost_{\pi m}, \quad (S26)$$

where MFV is the proportion of mass that veins make up of total leaf mass (g g^{-1}), CC_{leaf} is the leaf construction cost (g glucose g^{-1}) and LLS is leaf lifespan (d).

John, et al. [6] found *MFV* was approximately 0.25, while a crude mean CC_{leaf} and *LLS* can be obtained from averaging the pooled means of CC_{leaf} and *LLS* of the five plant life form types, and were found to be 1.49 g glucose g^{-1} and 211 d respectively. de Vries [8] estimated that the maintenance cost of osmotic pressure was on average approximately 8 mg glucose g^{-1} d^{-1}. From this, we can get

$$\frac{cost_{\mathrm{Kb}}}{cost_{\pi \mathrm{m}}} = \left(\frac{0.25 \times 1.49\ g\ glucose\ g^{-1}}{211\ d}\right) \Big/ 8\ mg\ glucose\ g^{-1}\ d^{-1} =$$

$$1.76\ mg\ glucose\ g^{-1}\ d^{-1} \Big/ 8\ mg\ glucose\ g^{-1}\ d^{-1} = 22\%,$$

which is close to the estimate based on the optimal model.

References

1 Cowan, I. in *Advances in botanical research* Vol. 4 117-228 (Elsevier, 1978).

2 Hari, P., Mäkelä, A., Korpilahti, E. & Holmberg, M. Optimal control of gas exchange. *Tree physiology* **2**, 169-175 (1986).

3 Lloyd, J. & Farquhar, G. D. ^{13}C discrimination during CO_2 assimilation by the terrestrial biosphere. *Oecologia* **99**, 201-215 (1994).

4 Lloyd, J. *et al.* A simple calibrated model of Amazon rainforest productivity based on leaf biochemical properties. *Plant, Cell & Environment* **18**, 1129-1145 (1995).

5 Buckley, T. N., Sack, L. & Farquhar, G. D. Optimal plant water economy. *Plant, Cell & Environment* **40**, 881-896 (2017).

6 John, G. P. *et al.* The anatomical and compositional basis of leaf mass per area. *Ecology Letters* **20**, 412-425, doi:10.1111/ele.12739 (2017).

7 Navas, M. L. *et al.* Leaf life span, dynamics and construction cost of species from Mediterranean old‐fields differing in successional status. *New phytologist* **159**, 213-228 (2003).

8 de Vries, F. W. T. P. The Cost of Maintenance Processes in Plant Cells. *Annals of Botany* **39**, 77-92, doi:10.1093/oxfordjournals.aob.a084919 (1975).